Benzilic acid as a template for photodimerization: Melting during photodimerization in a multicomponent solid

Mollah Rohan Ahsan,[a] Lavanya Singh,[a] Harshit Varma,[a] and Arijit Mukherjee *

Department of Chemistry,

Birla Institute of Technology and Science (BITS) Pilani, Hyderabad campus

Hyderabad. 500078, Telangana, India

Email ID: arijit.mukhejee@hyderabad.bits-pilani.ac.in

S1. Compounds used for this study: The compounds used for this study were benzilic acid (BZA), acridine (ACR), 4-iodopyridine (4-IPy), (E)-4-(3,5-dichlorostyryl) pyridine (**1**), (E)-4-(3-chlorostyryl) pyridine (**2**), (E)-4-(3-bromostyryl) pyridine (**3**). ACR was purchased from Sigma Aldrich, and 4-IPy was purchased from BLD pharm, both compounds were used without further purification. Other compounds were synthesized using the reported procedure. Detailed synthetic techniques and the scheme of the work are discussed below.

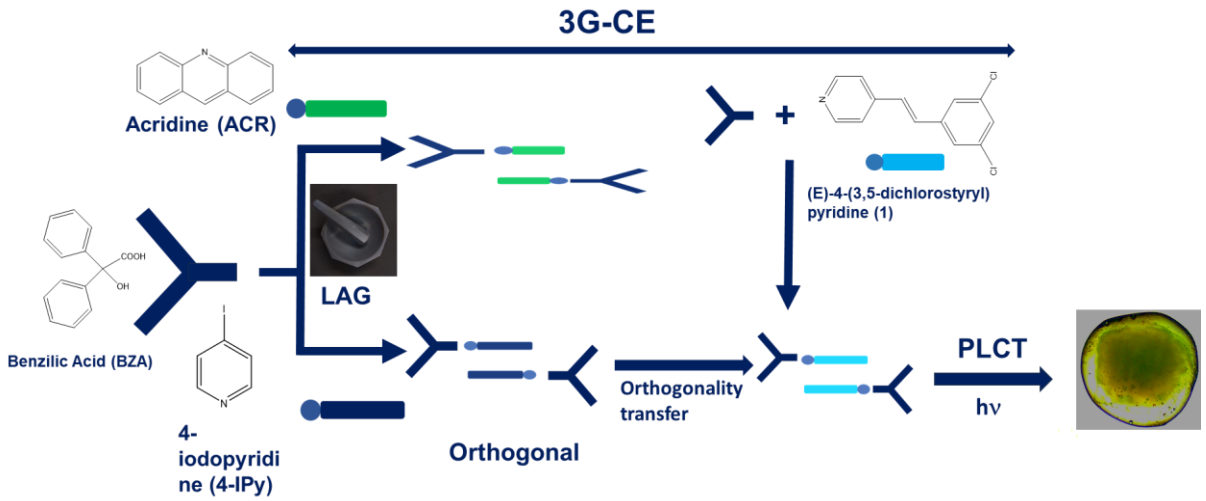

Scheme 1: Scheme representing different parts of the work.

Synthesis of chemical compounds:

A. Bezilic acid: Benzilic acid was synthesized using standard laboratory procedures.[1] 3.0 g of benzil and 9.0 mL of 95% ethanol were taken to a 100-mL round-bottom flask. The mixture was heated and stirred until the benzil dissolved. Then, 7.5 mL of an aqueous potassium hydroxide solution was added dropwise to the mixture. The mixture was refluxed for 15-20 minutes with stirring. The crude product was solidified and dissolved in hot water, and concentrated hydrochloric acid was added until the solution became acidic. The brownish-white solid obtained was washed thoroughly with cold water and crystallized from ethanol, and the recrystallized product was used for all the cocrystallization experiments.

B. (E)-4-(3,5-dichlorostyryl) pyridine (1): All the 4-stryrylpyridines used for this study were synthesized using a reported procedure.[2] 0.95 g of 4-methyl pyridine and 1.75 g of 3,5-dichlorobenzaldehyde was taken in 2 ml of acetic anhydride and stirred at 140^{o} C for 70-72 hours. The product was dissolved in 50-60 mL of dichloromethane after confirming complete conversion was observed through TLC (using 30% EtOAc/hexane solution). The crude product was transferred into a separating funnel. In the next step, 100 ml saturated sodium bicarbonate

solution was added. This process was repeated twice, and then the organic layer was filtered using anhydrous sodium sulfate. The solvent mixture was evaporated and crystallized from a mixture of DCM and hexane for further characterization.

C. (E)-4-(3-chlorostyryl) pyridine (2): 0.95 g of 4-methyl pyridine and 1.42g of 3-chlorobenzaldehyde was taken in 2 ml of acetic anhydride and stirred at 140^{o} C for 70-72 hours. The product was dissolved in 50-60 mL of dichloromethane after confirming complete conversion through TLC (using 30% EtOAc/hexane solution). The crude product was transferred to a separating funnel. In the next step, 100 ml saturated sodium bicarbonate solution was added.. This process was repeated twice, and then the organic layer was filtered using anhydrous sodium sulfate. The solvent was evaporated, and a dense, oily liquid was obtained that was crystallized through hexane wash.

D. (E)-4-(3-bromostyryl) pyridine (3): 0.95 g of 4-methyl pyridine and 1.75 g of 3-bromobenzaldehyde was taken in 2 ml of acetic anhydride and stirred at 140^{o} C for 70-72 hours. The product was dissolved in 50-60 mL of dichloromethane after confirming complete conversion through TLC (using 30% EtOAc/hexane solution). The crude product was transferred to a separating funnel, and 100 ml saturated sodium bicarbonate solution was added. This process was repeated twice, and then the organic layer was filtered using anhydrous sodium sulfate. The crude product was evaporated and crystallized from the hexane and DCM mixture for further characterization.

S2. Characterization of the synthesized compounds:

A. ^{1}H NMR spectra of the synthesized compounds: ~7 mg of the recrystallized sample was dissolved in $CDCl_3$, and NMR data was collected**.** NMR data confirms the formation of the product.

1

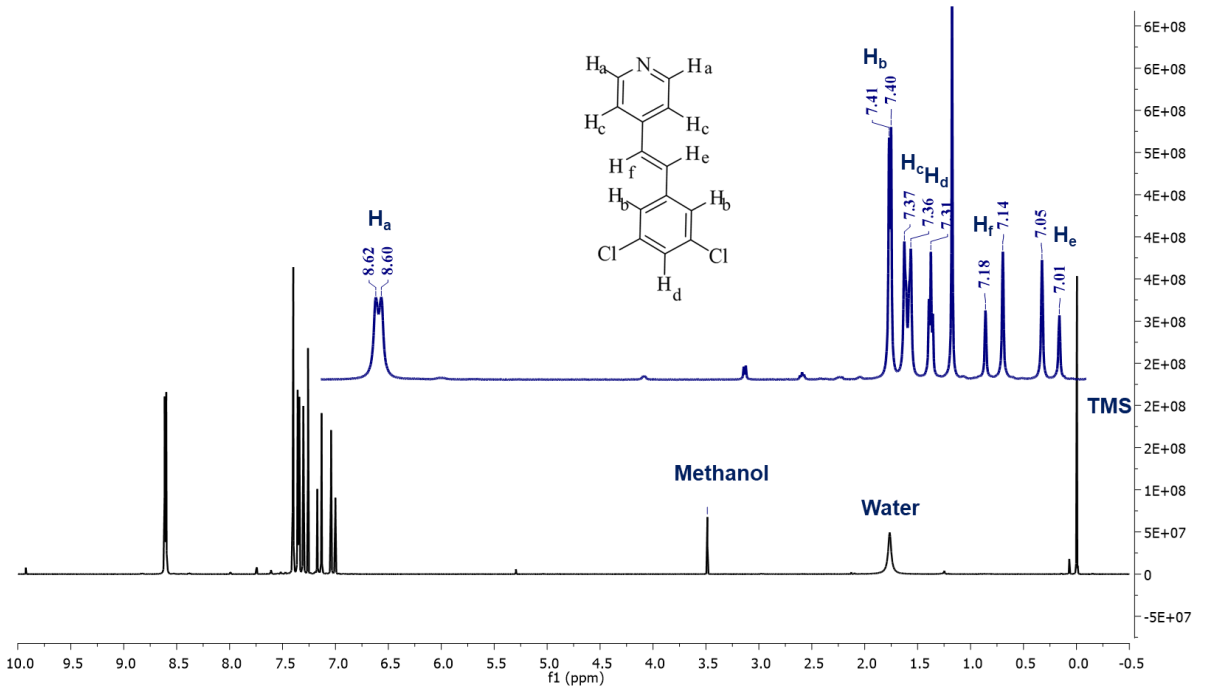
Ha
8.62
8.60
Hb
7.41
7.40
Hc Hd
7.37
7.36
7.31
Hf
7.18
7.14
7.05
He
7.01
TMS
Methanol
Water
f1 (ppm)

2

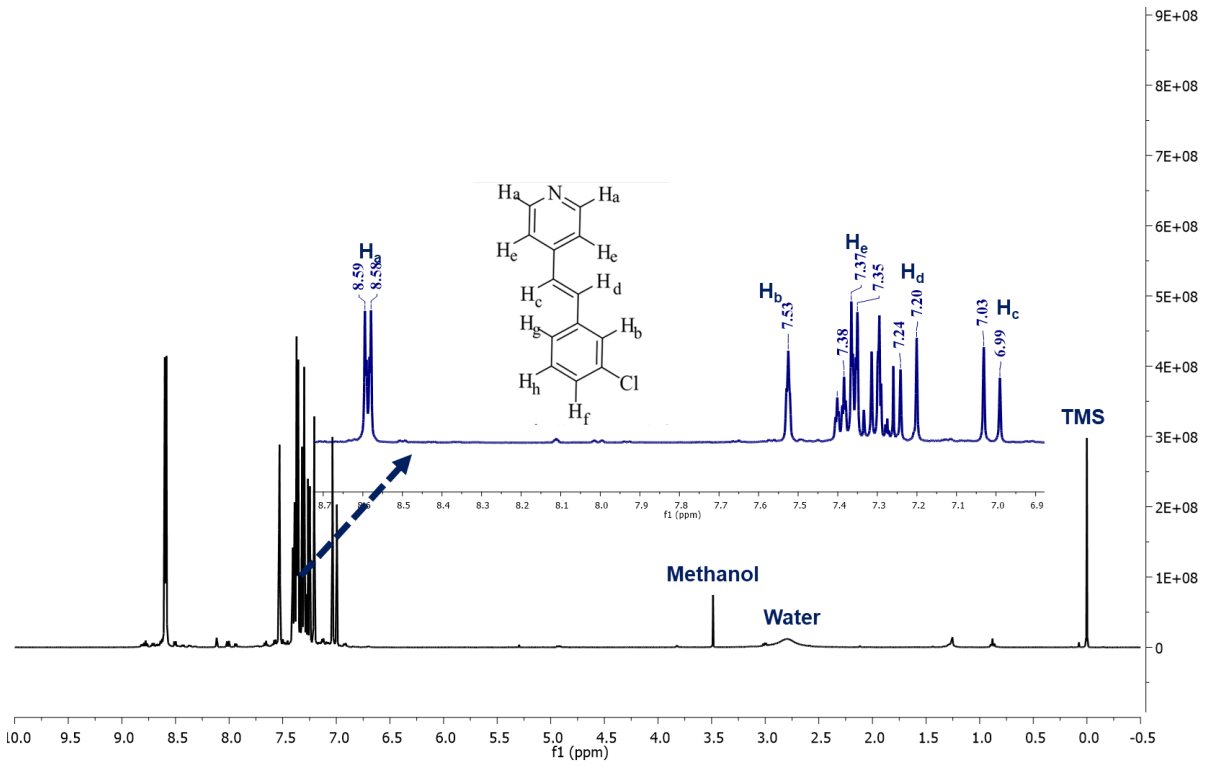
Ha
8.59
8.58
Hb
7.53
He
7.37
7.35
7.38
Hd
7.20
7.24
7.03
6.99
Hc
TMS
Methanol
Water
f1 (ppm)

3

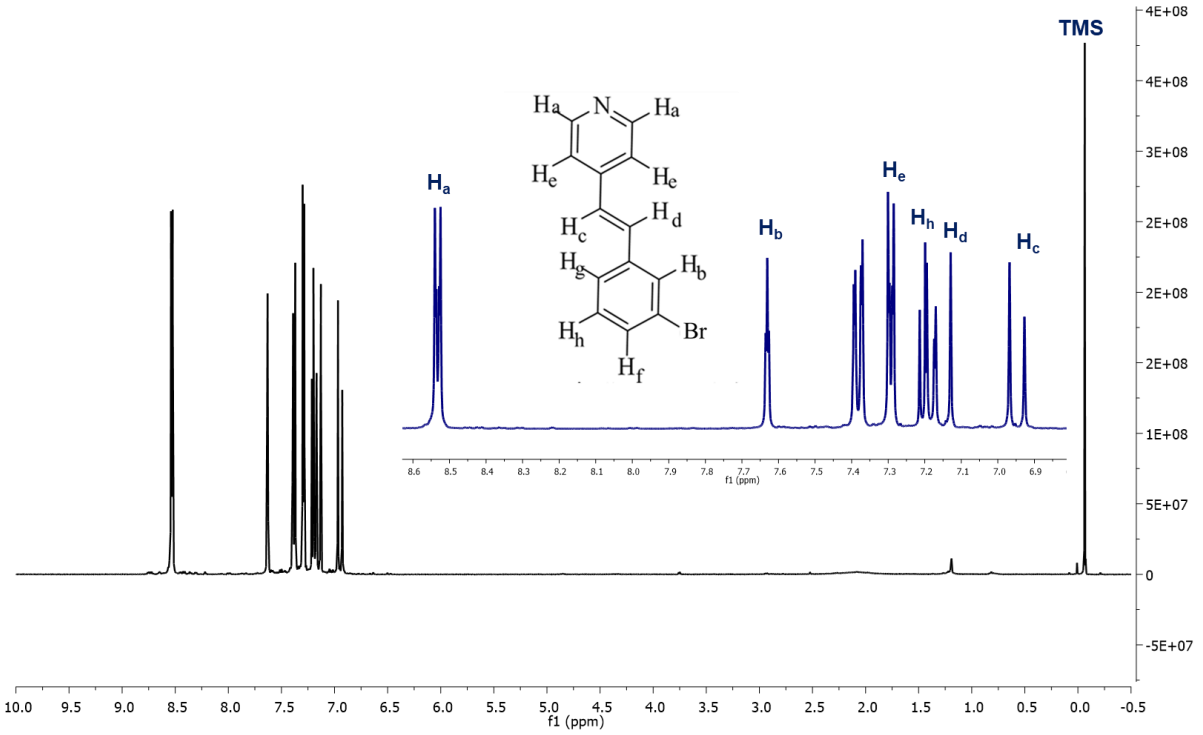

B. Mass spectra of the synthesized compounds: A pinch of the crystallized sample was dissolved in methanol, and mass spectra were collected using Shimadzu LCMS 8040. It is shown in the figure that the appearance of the peak in M+1 for all three compounds with nearly 100% abundance confirms the formation of the product.

1

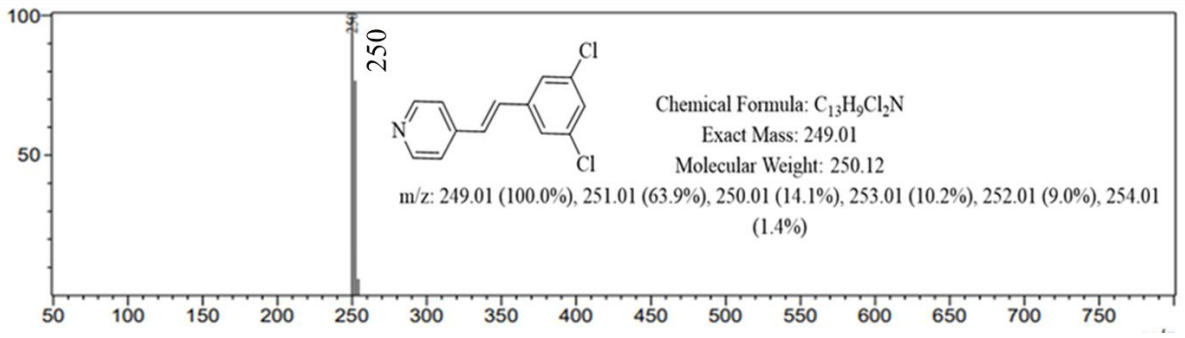

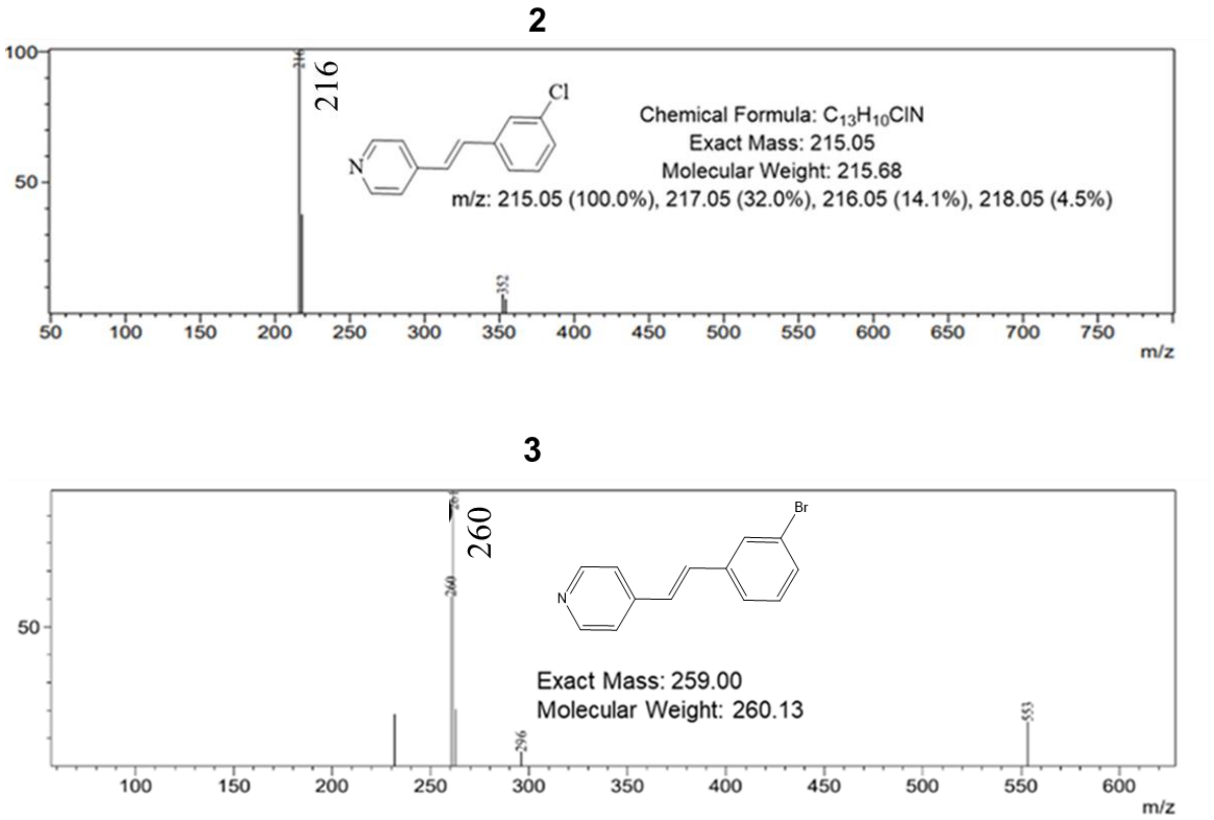

S3. CSD study:

A. CSD search for Benzilic acid cocrystals:

A CSD survey on Benzilic acid was carried out with Conquest 5.43 (November 2022) considering R-factor < 0.75, no polymers, no errors, no powder structures, and with organic structures only. Only three hits were obtained, out of which two were cocrystals. Among these two cocrystals, one forms a hydroxy-amine synthon along with O-H…O synthon with aniline. In another cocrystal system, Benzilic acid forms an O-H···O interaction with Cefradine, and the cocrystal crystallizes with methanol solvate. The reported cocrystals of Benzilic acid are shown below.

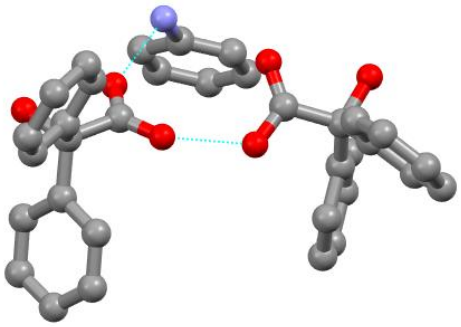	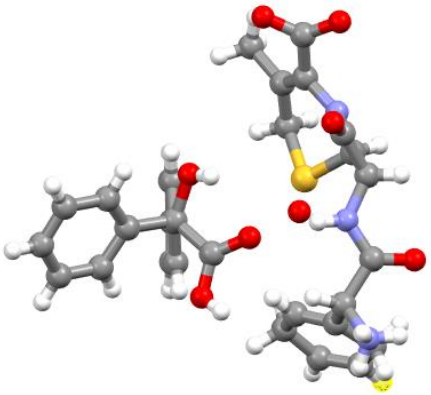
LAVZUF	VOQKAN

Figure 1: Reported cocrystals of Benzilic acid.

B. CSD study on 4-styrylpyridines used for photodimerization

Another CSD search was done on 4-styrylpyridines using the same version of CSD using the same criteria used in the previous search (R-factor < 0.75, no polymers, no errors, no powder structures and with organic structures only). Two hundred sixty-seven hits were obtained when we searched for 4-styryl pyridine fixing the hydrogens in the olefinic position. Of these, 119 are single components, 123 are cocrystals or solvated cocrystals, and 25 are solvated native structures. **Amongst 123 cocrystals, 40 cocrystals undergo photochemical reactions.** When a search was done in Conquest 5.43 (November 2022) for 4-styrylpyridinium molecule with R-factor < 0.75, no polymers, no errors, no powder structures, with organic structures only, and with number of molecules >1. 59 hits were obtained, out of which 32 are hydrate or solvate that crystallized with some anion, mostly with Cl^- anion; out of the remaining 22 are multicomponent crystals or solvated multicomponent crystals (*where at least 2 components are solid in room temperature*), 17 were utilized for photochemical reaction, only 8 cases were found where template strategy utilized successfully. Amongst these 58 cocrystals or salts, only four thiourea, resorcinol derivatives, boronic ester, and 1,2,4,5-benzene tetracarboxylic acids were implemented successfully as a template.

Ref code	coformer	styrylpyridine
APEDUV APEFAD APEFEH APEFIL	Thiourea[3]	1-(4-Pyridyl)-2-(4-cyanophenyl)ethylene 1-(4-Pyridyl)-2-(phenyl)ethylene 4-(2-(4-fluorophenyl) vinyl) pyridine

APEFOR APEFUX APEGAE APEGEI APEGIM APEGOS		4-(2-(4-Chlorophenyl) vinyl) pyridine 4-(2-(4-bromophenyl) vinyl) pyridine 4-(2-(4-Methylphenyl)vinyl)pyridine 4-(2-(4-Methoxyphenyl)vinyl)pyridine 4-(2-(2,4-Dichlorophenyl)vinyl)pyridine 1-(4-Pyridyl)-2-(4-ethylphenyl)ethylene 4-(2-(2-Naphthyl)vinyl)pyridine
GATZIM GAVBEM GAVBIQ GAVBOW	4,6-dibromobenzene-1,3-diol[4]	bis(Methyl 4-(2-(pyridin-4-yl)vinyl)benzoate
GUZTOM08 GUZTOM09 GUZTOM10 GUZTOM11	4,6-dichlorobenzene-1,3-diol[5]	bis(methyl 4-(2-(pyridin-4-yl)vinyl)benzoate)
HAFSUF HAGHOP	Urea[6]	4-(2-(4-Chlorophenyl) vinyl) pyridine 1-(4-Pyridyl)-2-(4-cyanophenyl)ethylene
ITODON- ITOFAB	No coformer [7]	1,1'-(ethene-1,2-diyl)bis(2,3,5,6-tetrafluorobenzene) and 4-(2-phenylethenyl)pyridine
ITUJAJ ITUJIR ITUJOX	5-iodobenzene-1,3-diol[8]	4'-(2-Phenylvinyl)-2,2':6',2''-terpyridine benzene-
KAQCOW- KAQCUC	resorcinol[9]	4-(2-(4-methylphenyl)vinyl)pyridine 4-[2-(4-chlorophenyl)ethenyl]pyridine
NOTFOU NOTFOU01 NOTFOU02 NOTFOU03 NOTFOU04	(1,2,4,5-tetrachloro-3,6-diiodobenzene)[10]	1-(4-Pyridyl)-2-(phenyl)ethylene
POWREB	4,6-diiodobenzene-1,3-diol[11]	bis(4-[2-(pyridin-4-yl)ethenyl]phenyl) acetate

VIVXIK VIVXOQ VIVXUW	4,6-dibromobenzene-1,3-diol 4,6-dichlorobenzene-1,3-diol (solid solution)[12]	1-(4-Pyridyl)-2-(phenyl)ethylene
YICLAA	4,6-dichlorobenzene-1,3-diol[13]	1-(4-Pyridyl)-2-(phenyl)ethylene
YIXKUO JUTLUI	Boronic Ester[14,15]	1-(4-Pyridyl)-2-(phenyl)ethylene 1-(4-pyridyl)-2-(2-thienyl)ethylene
ABELOI	5-methoxyresorcinol[16]	1,4-bis(2-(4-pyridyl)ethenyl)benzene
TEXBEG TEXBOQ TEXBUW TEXCAD TEXCIL TEXCOR TEXCOR01 TEXBAC01 RACSUL	1,2,4,5-benzene tetracarboxylic acids[17]	4-[2-(4-cyanophenyl)ethenyl]pyridin-1-ium) 4-[2-(2,4-dichlorophenyl)ethenyl]pyridin-1-ium 4-[2-(3-bromophenyl)ethenyl]pyridin-1-ium) 4-[2-(4-bromophenyl)ethenyl]pyridin-1-ium 4-[2-(2-cyanophenyl)ethenyl]pyridin-1-ium 4-[2-(2-chlorophenyl)ethenyl]pyridin-1-ium 4-[2-(2-chlorophenyl)ethenyl]pyridin-1-ium 4-[2-(3-chlorophenyl)ethenyl]pyridin-1-ium 1-Phenyl-2-(pyridin-1-ium-4-yl)ethene
UDISOS	4-carboxy-2,3,5,6-tetrafluorobenzoate[18]	4-[2-(naphthalene-1-yl)ethenyl]pyridin-1-ium
ILAPOD ILAPIX	2,3,5,6-tetrafluorobenzoate[19] 2,3,5,6-tetrafluoro-4-hydroxybenzoate[19]	4-[2-(naphthalene-1-yl)ethenyl]pyridin-1-ium

DUQWUK	(1-oxo-1H-2-benzopyran-3-carboxylic acid)[20]	1,8-bis(4-pyridinioethenyl)naphthalene
WULZUB WUKFIU	Oxalic acid[21]	4-(2-phenylethenyl)pyridinium 4-(2-phenylethenyl)pyridinium
UMEDIC UMEDIC01	hexafluorophosphate[22]	4-(2-phenylethenyl)pyridinium 4-(2-phenylethenyl)pyridinium

C. Studying torsional preference (C-N⋯O-C) in pyridine derivatives and acridine while cocrystallized with a coformer

Varying torsional preference was observed for pyridine and acridine moiety when we searched in CSD. When a search was performed for cocrystals with acid-pyridine synthon for the torsion angle (C-O⋯N-C) and contact N⋯H by considering R-factor < 0.75, no polymers, no errors, no powder structures, and with organic structures only, 2052 hits were obtained. When the obtained structures were plotted with Torsion vs. Distance (N⋯H), the torsional angle was concentrated at 0° and 180°, which defines that carboxylic acid prefers planar orientation for pyridine moieties. Then, another search was performed for cocrystals of acridine having acid pyridine synthon for torsional preferences without adding hydrogen to the backbone of acridine. 32 hits were obtained, out of which only 7 are within the range of 0-50 and 130-180; the rest preferred orthogonal or near orthogonal orientation. Similar fondness of torsional angle was observed for carboxylate-pyridinium and carboxylate-acridinium synthons.

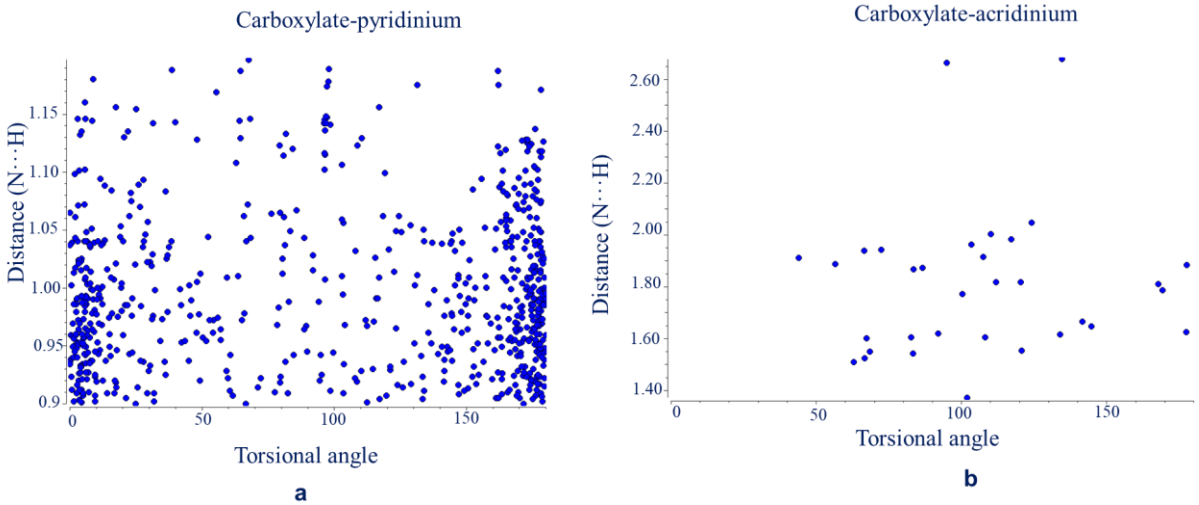

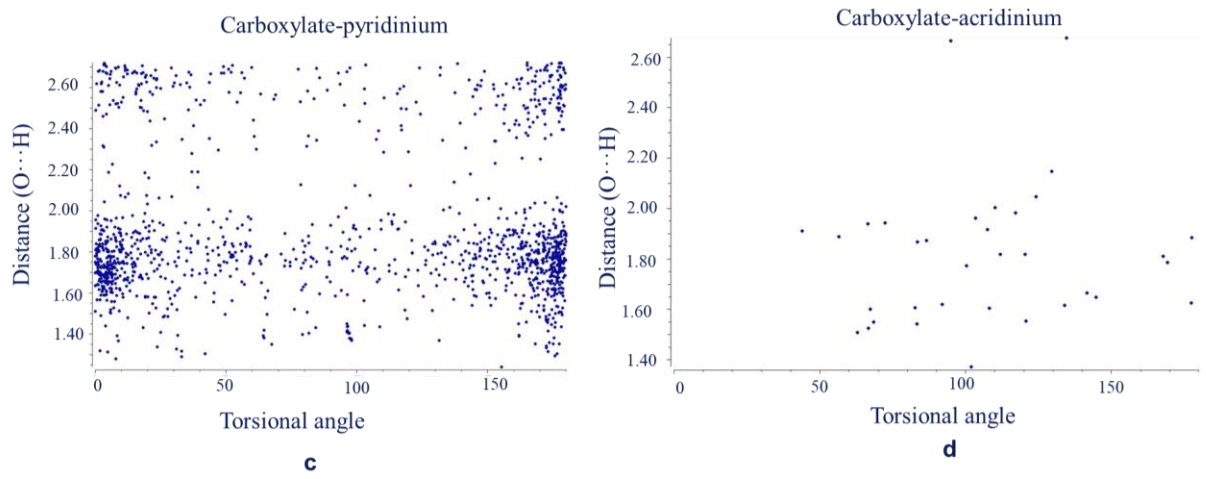

Figure 2: Scatter plot of torsion C-N-O-C vs contact (N···H and O···H) for the CSD search of (a) acid-pyridine (b) acid-acridine and acridine derivatives, (c) carboxylate-pyridinium, (d) carboxylate-acridinium.

S4. Infrared Spectroscopy (IR-Spectra):

The samples BZA, BZA-ACR, BZA-4-IPy 1.BZA were prepared as mentioned in the synthesis and crystallization section. Grind mixture of these recrystallized samples were used to collect IR-spectra using Bruker ATR instrument within a range of 500 to 4000 cm^{-1} with a resolution of 4 cm^{-1}. The carbonyl stretching frequency lowered from BZA to BZA-4-IPy to 1.BZA lowest frequency was observed for BZA-ACR. This observation confirmed the weakening of the C=O bond. Carbonyl bond order could decrease when there was a possibility of proton transfer. The carbonyl bond length of the refined benzilic acid structures were also supported the IR observation. The carbonyl bond length and IR frequency for carbonyl stretching are tabulated below. To further confirm the observations from IR-spectra and carbonyl bond length of the refined structures, computational calculations were also performed; for details see ESI-S5.

compound	C=O (D2) (Å)	C-O (D1) (Å)	ΔD= D2 - D1 (Å)	C=O stretching frequency (cm^{-1})
BZA native structure	1.213(6)	1.301(5)	0.088	1705
BZA-4-IPy	1.219(4)	1.297(5)	0.078	1695
1.BZA	1.224(3)	1.273(3)	0.049	1687

BZA-ACR	1.239(2)	1.269(2)	0.03	1657

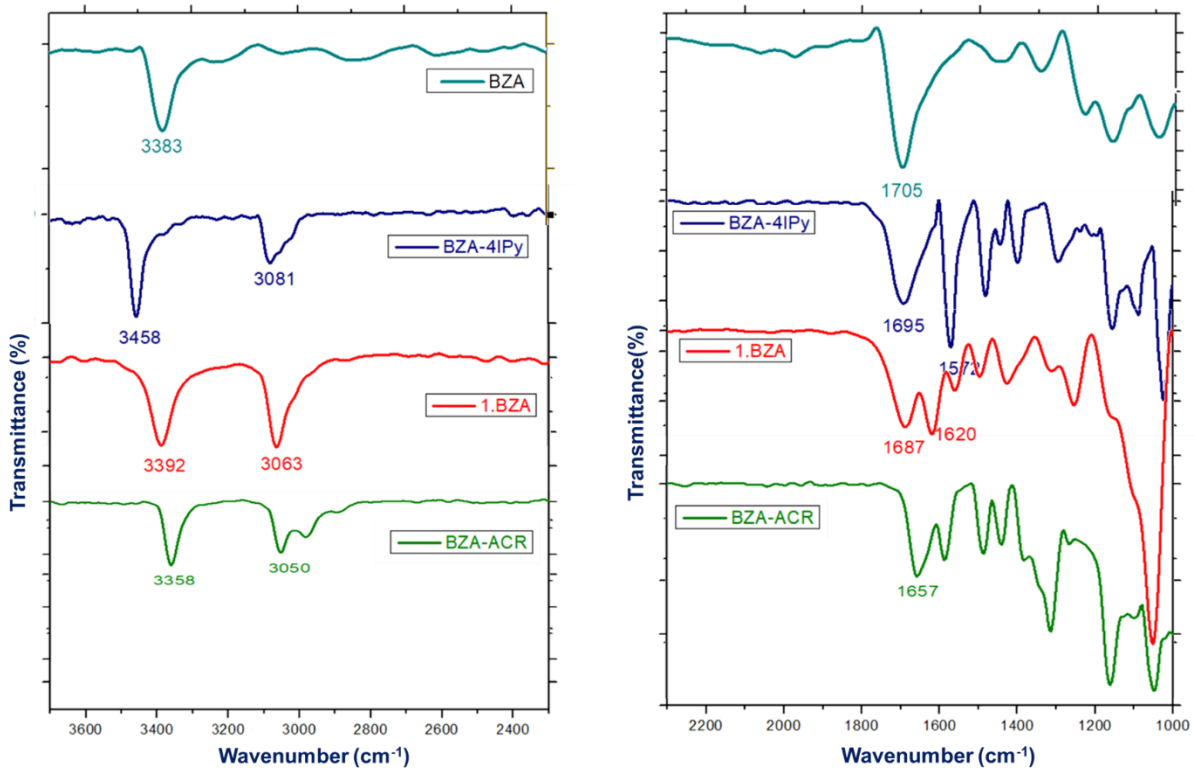

Figure3. IR spectra of (a) benzilic acid, (b) BZA-4-IPy, (c) 1.BZA, (d) BZA-ACR.

S5. Computational studies:

A. ΔpKa calculation

Δpk_a calculation is generally used as a guideline to recognize cocrystals, continuum, and salt formation for multicomponent crystals comprising acids and bases.[23] Δpk_a calculation for the coformers was done using ChemAxon Chemicalize software. pk_a for the conjugate acid of the base and pk_a for the acid was tabulated below, and Δpk_a is also calculated. Almost 0.86 pk_a difference between the two coformers observed with benzilic acid. ACR has a higher pk_a value compared to 1, which defines the higher tendency of ACR for proton transfer.

Compound	Pk_a	Δpk_a
BZA	3.93	-------
Conjugate acid of ACR	6.15	2.22
Conjugate acid of 1	5.29	1.36

B. ESP calculation of ACR and 1:

ESP calculations for acridine and *(E)-4-(3,5-dichlorostyryl) pyridine* were carried out using Gaussian 09. The DFT-based method was used to calculate the ESP charges using the basis set B3LYP 6311G* with the keyword pop=chelpg. After completion of the calculation, the ESP maps were generated by using molecular electron density of 0.0004 electron/Å. The respective colour codes mark the locations of positive charges as green and negative charges as red surfaces. The charge on the N atom of ACR is -0.855368, which is much higher than the charge concentrated on the N atom of 1. Depending on the charges of the respective molecule that concentrates on the N-atoms, it is clear that ACR possesses a higher negative charge than 1 (-0.815475), which hinted at the salt formation tendency of ACR over 1.

Molecule	Template Energy (Hartree)	Mullikan Charges	ESP charges
ACR	-551.794334	1 C -0.076703	1 C -0.098915
		2 C -0.094884	2 C -0.227449
		3 C 0.676125	3 C 0.076637
		4 C -0.833328	4 C 0.611176
		5 C -0.479563	5 C -0.301625
		6 C -0.267230	6 C -0.069125
		7 C 0.099651	7 C -0.298013
		8 C -0.833328	8 C 0.611176
		9 C 0.676125	9 C 0.076637
		10 C -0.094884	10 C -0.227449
		11 H 0.251491	11 H 0.129323
		12 C -0.076703	12 C -0.098915
		13 C -0.267230	13 C -0.069125
		14 C -0.479563	14 C -0.301625
		15 H 0.269079	15 H 0.196708
		16 H 0.235811	16 H 0.100817
		17 H 0.251491	17 H 0.129323
		18 H 0.265988	18 H 0.149879
		19 H 0.240104	19 H 0.107618
		20 H 0.235811	20 H 0.100817

		21 H 0.240104 22 H 0.265988 23 N -0.204354	21 H 0.107618 22 H 0.149879 23 N -0.855368
1	-1475.760554	1 C 0.316535 2 C -0.395775 3 C -0.530282 4 C -0.232511 5 C 0.605297 6 C -1.107789 7 H 0.182644 8 H 0.196297 9 H 0.212541 10 C -0.362676 11 C -0.474944 12 H 0.164566 13 H 0.161636 14 C -0.051768 15 C 0.001760 16 C 0.768703 17 C -0.430017 18 H 0.167063 19 C -0.412481 20 H 0.179689 21 N -0.200214 22 H 0.186093 23 H 0.186822 24 Cl 0.428875 25 Cl 0.439936	1 C 0.148005 2 C -0.157723 3 C 0.137908 4 C -0.218177 5 C 0.181305 6 C -0.151045 7 H 0.114544 8 H 0.135171 9 H 0.134580 10 C -0.087524 11 C -0.411009 12 H 0.135004 13 H 0.213164 14 C 0.590035 15 C -0.523864 16 C -0.546249 17 C 0.582903 18 H 0.146221 19 C 0.601032 20 H 0.150580 21 N -0.815475 22 H -0.020292 23 H -0.023860 24 Cl -0.154784 25 Cl -0.160450

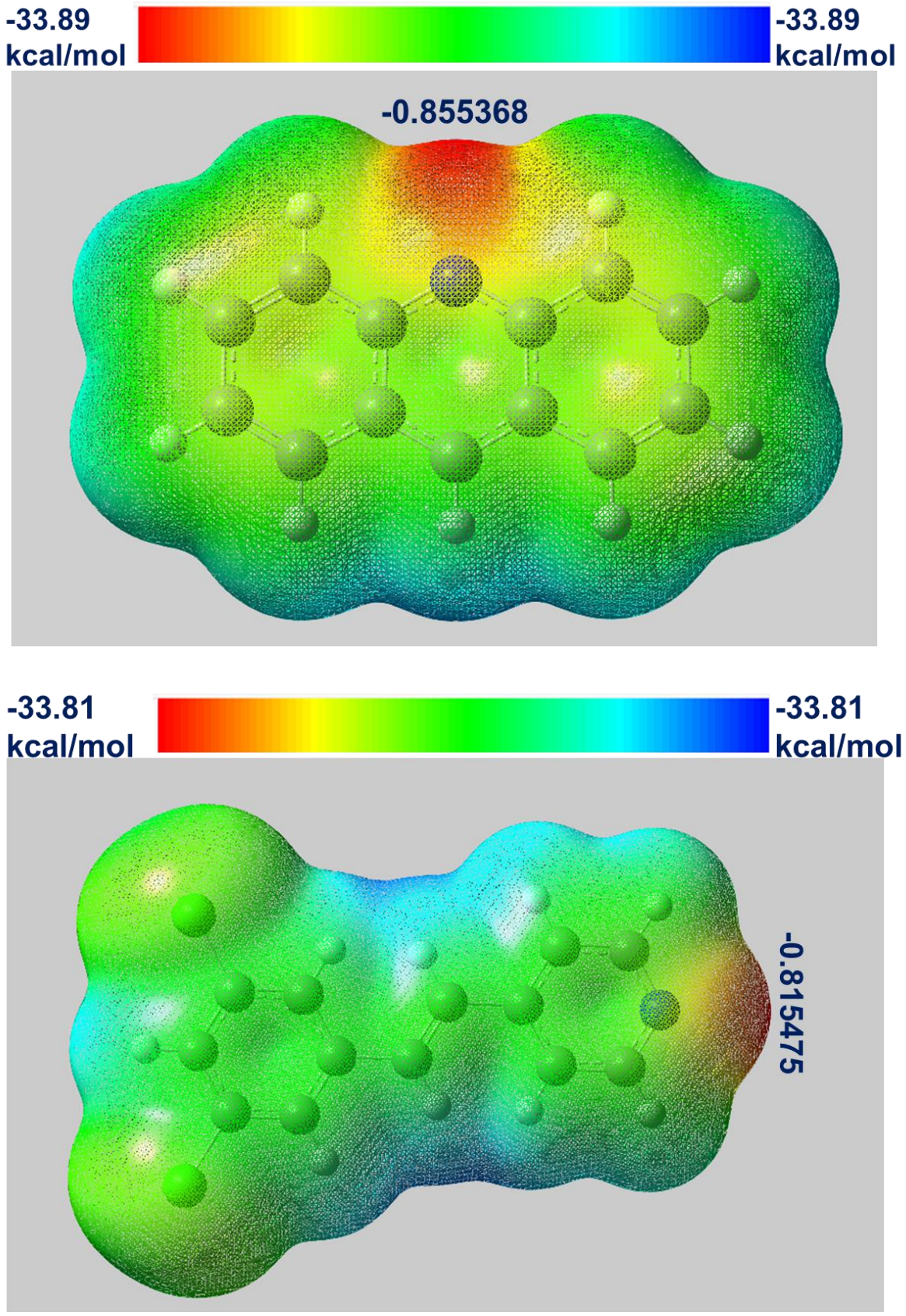

Figure 4: Electrostatic surface potential of (a) ACR and (b) 1.

C. Slant Plane Calculation: The slant plane of three systems, BZA-ACR, BZA-4IPy, and 1.BZA, were calculated by removing labile hydrogen from the structure using WinGX software[24]. Plane containing carboxylic O and pyridine N was considered for generating the plane. The gradual shifting of residual density toward N from 4-IPy to 1 to ACR indicated the more salt character of the BZA-ACR system.

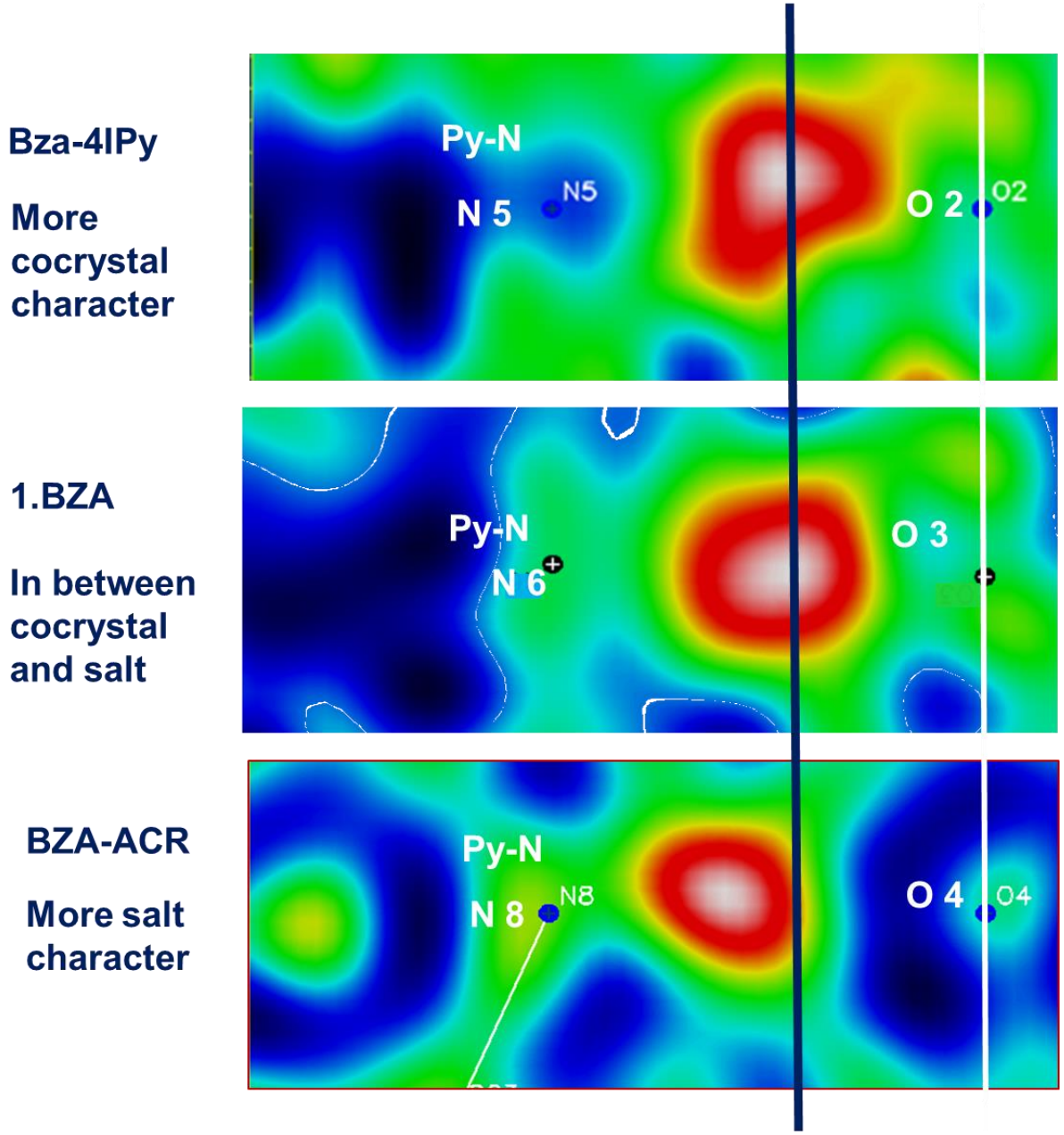

D. Energy Framework calculation

Energy framework calculation was performed using Crystal Explorer 21.5[25] using a B3LYP 6311G(d,p) basis set. The weakest interaction for 1 was observed along the (011) plane. The weakest interaction for 1 and 2 is marked with blue and red patches.

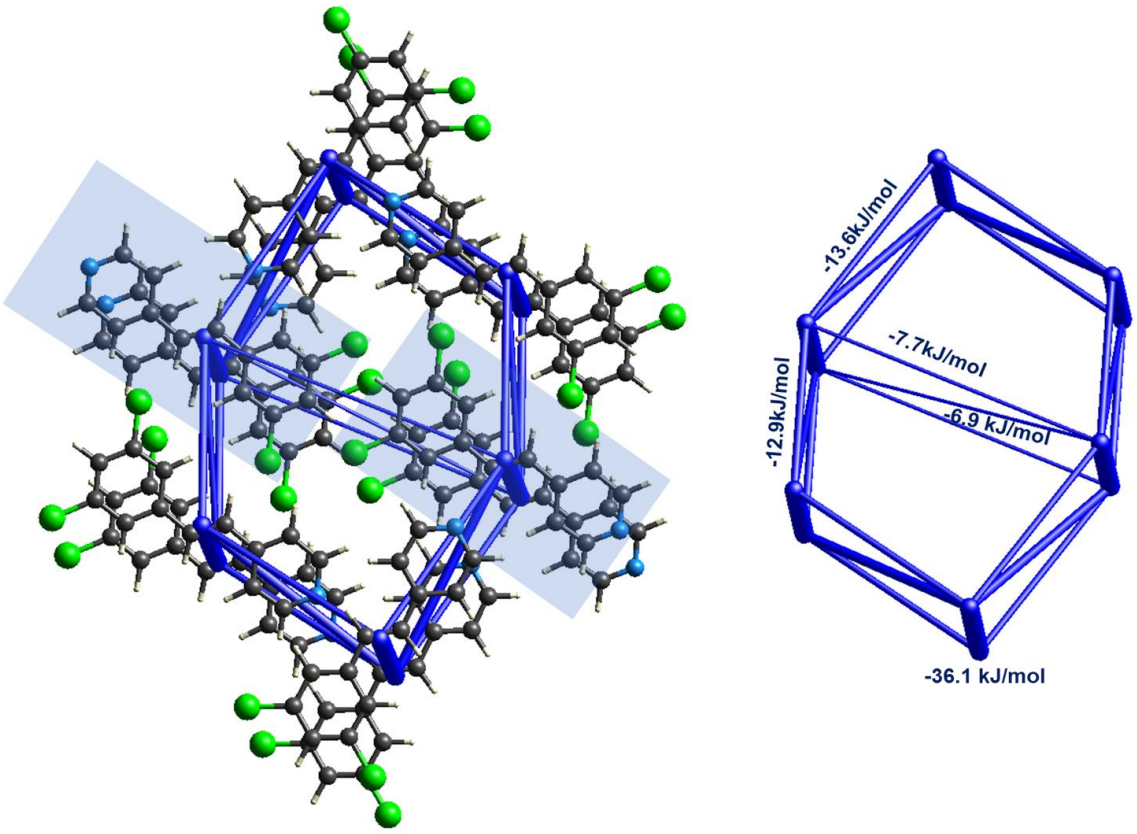

(a)

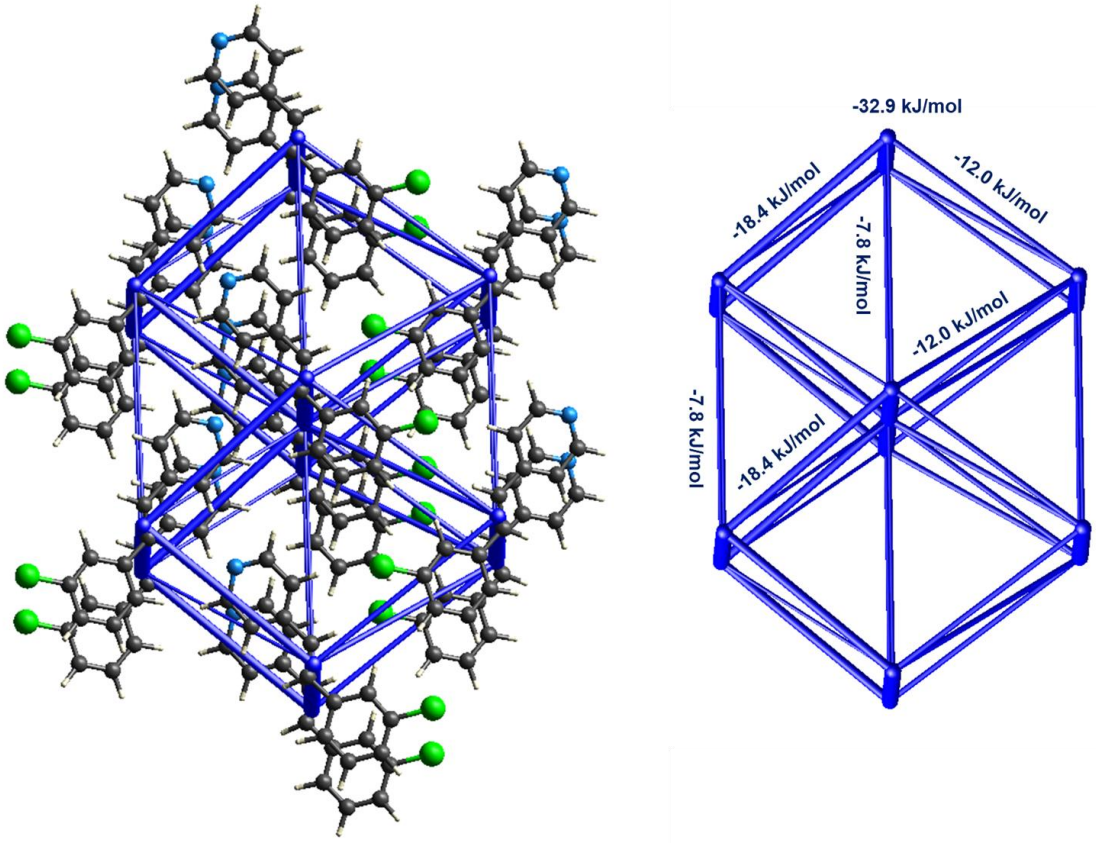

(b)

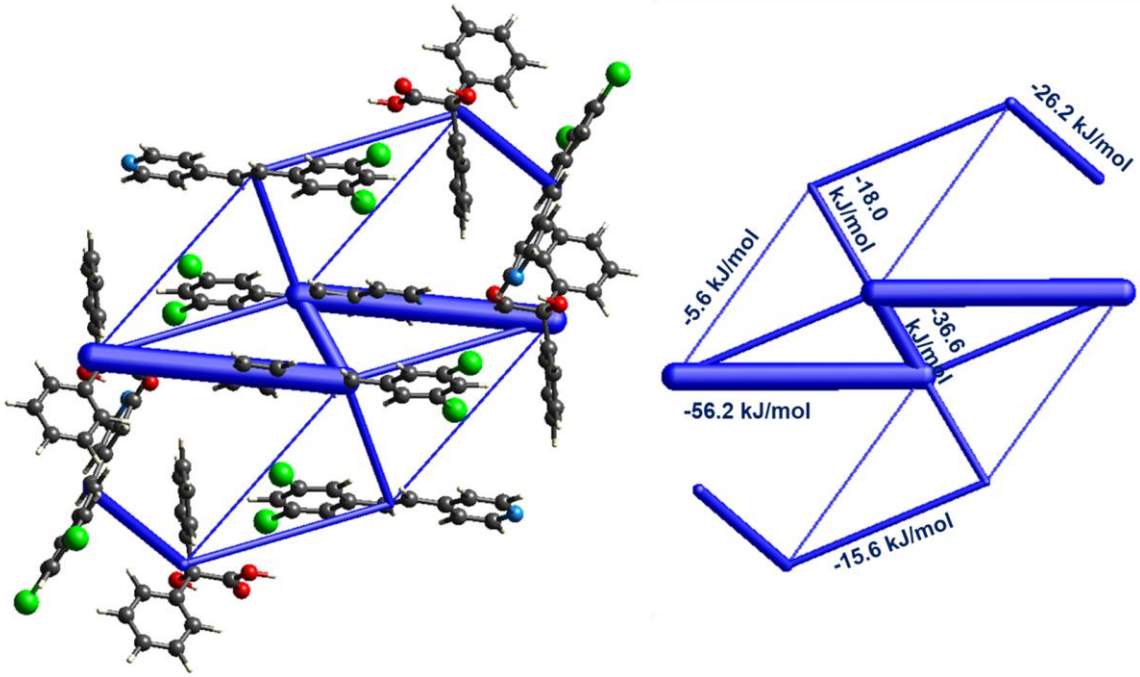

(c)

Figure 5: Energy framework analysis for (a) 1, (b) 2, (c) 1.BZA

S6. Crystallization Details

(a) Crystallization procedure of BZA.ACR: Three coformers, benzilic acid (~57mg), 4,4′-bipyridine (~ 39 mg), and acridine (~45mg) were taken in a 1:1:1 ratio in a mortar and ground with 5-6 drops of DCM three times. The DCM ground mixture was then dissolved in ethanol and kept for evaporation. After 4 days, yellow-colored block-shaped crystals were obtained and used for single crystal analysis.

(b) Crystallization procedure of BZA.4IPy: Benzilic acid (~57mg) and 4-iodopyridine (~51.2mg) were taken in a 1:1 ratio and ground with ethanol (5-6 drops) three times. The ethanol ground mixture was dissolved in nitromethane and kept for slow evaporation. Colorless block-shaped crystals were obtained after 4 days.

(c) *Crystallization procedure of 1.BZA:* (E)-4-(3,5-dichlorostyryl) pyridine(~62.5mg) and benzilic acid (~57 mg) were taken in 1:1 ratio and ground with DCM 3-4 times. The DCM ground powder mixture was dissolved in DCM and kept for slow evaporation. Yellow block-shaped crystals were obtained after 2 days. These crystals were used for further characterization and photo irradiation.

(d) *Crystallization procedure of 2.BZA:* (E)-4-(3-chlorostyryl) pyridine(~54mg) and benzilic acid (~57 mg) was taken in 1:1 ratio and ground with DCM 3-4 times. The DCM ground mixture was dissolved in DCM and kept for slow evaporation. Yellow block-shaped crystals were obtained after 2 days and used for further characterization and photo irradiation.

(e) *Crystallization procedure of 3.BZA:* (E)-4-(3-bromostyryl) pyridine(~65mg) and benzilic acid (~57 mg) was taken in 1:1 ratio and ground with DCM 3-4 times. The ground mixture was dissolved in DCM and kept for slow evaporation. Yellow block-shaped crystals were obtained after 2 days and used for further characterization and photo irradiation.

S7. Single Crystal X-ray diffraction:

All the single crystal data were collected *using Rigaku* Oxford XtaLAB diffractometer using Cu-Kα (λ= 1.54184 Å) radiation, and the collected data were processed with CrysAlisPRO 2015 software. Some data reductions were performed using CrysAlisPro 2021. The structure solution was carried out with the SHELXT program, and data refinement was done using SHELXL programs embedded in OLEX^2-1.51. All non-hydrogen atoms were refined anisotropically by the full-least-squares method, whereas all the hydrogen atoms were refined isotopically. The H atoms were fixed on a riding model, and acidic H atoms were located via

Fourier maps. Mercury version 4.2.0[26] was used for crystal structure analysis and for generating packing diagrams. The Packing diagram of BZA.ACR, BZA-4IPy, 1 and 1. BZA was presented in the manuscript, packing diagram of 2, 3, 2.BZA and 3.BZA is shown below.

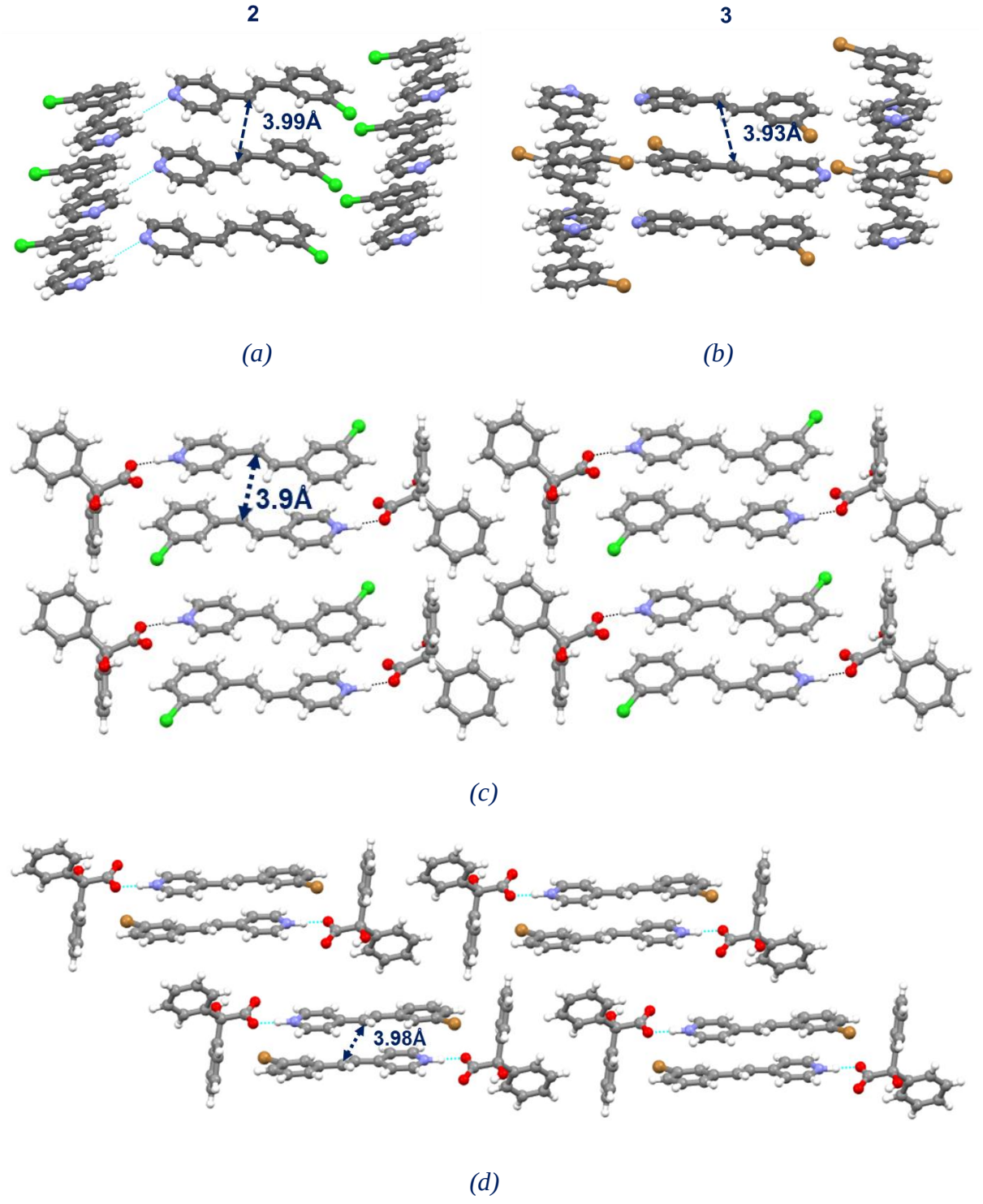

Figure 6: Packing diagram of (a) 1, (b) 2, (c) 2.BZA (d) 3.BZA.

S8. (a) Crystallographic table:

compound	BZA.ACR	BZA-4IPy	1	2
Empirical formula	C_{27} H_{21} N O_3	C_{19} H_{16} I N O_3	C_{13} H_9 Cl_2 N	C_{13} H_{10} Cl N
CCDC NO.	2289890	2289891	2290412	2291018
Formula Weight	407.45	433.23	250.11	215.67
Crystal System	Triclinic	Triclinic	Monoclinic	Monoclinic
Space Group	$P\bar{1}$	$P\bar{1}$	$P2_1/c$	*P*n
a (Å)	6.7453(2)	6.4536(1)	3.8714(1)	3.9947(2)
b (Å)	16.8984(3)	8.3751(2)	11.4217(3)	13.9322(5)
c (Å)	18.0463(4)	16.1607(5)	26.3704(6)	9.8346(4)
α (˚)	93.589(2)	83.149(2)	90	90
β (˚)	94.776(2)	86.845(2)	89.998(2)	100.133(4)
γ (˚)	99.891(2)	83.349(2)	90	90
V (Å3)	2013.19(8)	860.65(4)	1166.05(5)	538.81(4)
ρ_{calc} ***(g/cm3)***	1.344	1.672	1.425	1.329
F (000)	856.0	428.0	512.0	224.0
μ. (mm-1)	0.701	14.757	4.743	2.817
T (K)	140	140	295	300
λ (Å)	1.54184	1.54184	1.54184	1.54184
Total Reflections.	8483	3605	2483	1684
Unique Reflection	6467	3506	2141	1576
Completeness (%)	99.7	99.4	99.7	99.9
R_{int}	5.27	4.37	5.84	3.01
R_1 (F^2)	5.11	3.99	4.53	3.57
$wR_2(F^2)$	14.77	11.21	13.94	10.33
GoF	1.066	1.074	1.062	1.053
Θ_{max}	79.662	79.796	79.367	79.682
compound	3	1.BZA	2.BZA	3.BZA
Empirical formula	C_{13} H_{10} Br N	C_{27} H_{21} Cl_2 N O_3	C_{27} H_{22} Cl N O_3	C_{27} H_{22} Br N O_3
CCDC NO.	2291142	2289881	2289888	2289889

Formula Weight	260.12	478.35	443.91	488.36
Crystal System	Orthorhombic	Monoclinic	Triclinic	Triclinic
Space Group	$P\ 2_12_12_1$	$P2_1/c$	$P\bar{1}$	$P\bar{1}$
a (Å)	7.3605(4)	8.9426(3)	8.5593(2)	8.79940(10)
b (Å)	12.2746(4)	18.2781(4)	10.3705(2)	10.2996(1)
c (Å)	12.3726(3)	14.4279(4)	13.0745(2)	13.0538(2)
α (°)	90	90	88.6790(10)	89.3630(10)
β (°)	90	90.619(2)	74.542(2)	74.7030(10)
γ (°)	90	90	82.8740(10)	82.8310(10)
V (Å3)	1117.83(8)	2358.16(12)	1109.87(4)	1131.94(2)
ρ_{calc} ***(g/cm3)***	1.546	1.347	1.328	1.433
F (000)	520.0	992.0	464.0	500.0
μ. (mm-1)	4.705	2.715	1.760	2.708
T (K)	295	140	140	143
λ (Å)	1.54184	1.54184	1.54184	1.54184
Total Reflections	2153	5016	4648	4746
Unique Reflections	1510	3264	4256	4386
Completeness (%)	99.6	100	99.7	99.6
R_{int}	4.45	4.58	3.37	3.02
$R_1\ (F^2)$	5.54	5.47	3.96	4.10
$wR_2(F^2)$	18.32	16.26	10.76	11.77
GoF	1.081	1.058	1.106	1.106
Θ_{max}	79.905	79.779	79.754	79.457

(b) H-bonding table:

structure	interaction	D-H	H···A (Å)	D···A (Å)	<(DHA) (°)
BZA-ACR	N8-H8···O4	1.06(3)	1.53(3)	2.5792(18)	168(2)
	N7-H7···O1	1.04(3)	1.54(3)	2.5687(18)	168(2)
	O6-H6···O5	0.96(3)	1.87(3)	2.5481(18)	125(2)
	O3-H3···O2	0.90(3)	1.97(3)	2.589(2)	124(2)
BZA-4-IPy	O4-H4···O3	0.90(7)	1.98(7)	2.596(4)	124(5)

	O2-H1···N5	1.03(8)	1.55(3)	2.554(4)	165(7)
1.BZA	O5-H5···O4	0.73(4)	2.07(4)	2.577(3)	127(4)
	O2-H1···N5	1.18(4)	1.36(4)	2.534(2)	173(4)
2.BZA	O4-H4···O3	0.87(2)	1.87(2)	2.5312(15)	131(2)
	N5-H2···O2	1.10(3)	1.46(3)	2.5555(14)	173(2)
3.BZA	O18-H18···O17	0.63(4)	2.04(4)	2.539(3)	136(4)
	N1-H1···O16	1.03(6)	1.54(6)	2.553(2)	170(5)

S9. Characterization of the crystallized sample

A. Powder X-ray Diffraction (PXRD) analysis:

PXRD for the native compound and cocrystals were collected using ground recrystallized samples prepared as discussed before. PXRD for all the cocrystals were collected using Rigaku Ultima IV in a 2θ range of 5-35° with a scan speed of 2°/min using a step size of 0.01. All the simulated PXRD patterns are generated using Mercury 4.2.0[26] software, and the stacked PXRD plots were prepared using X'pert HighScore Plus software.

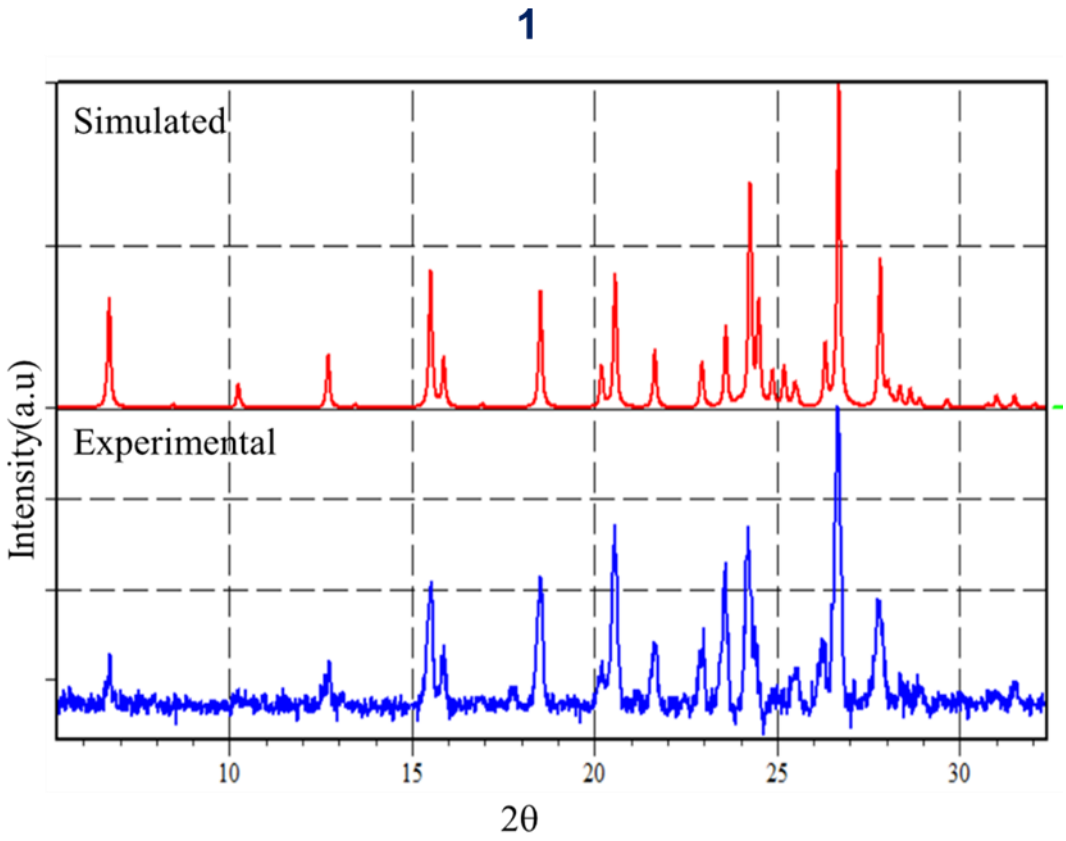

2

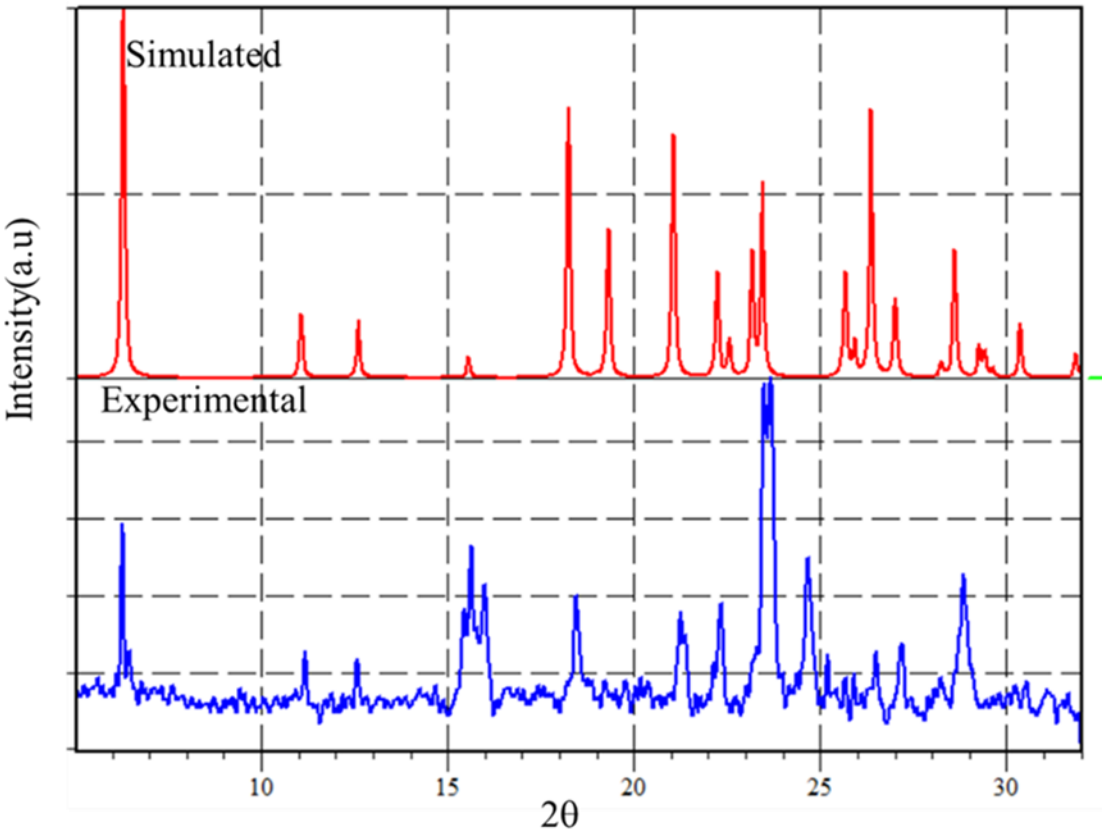
Simulated
Experimental
Intensity(a.u)
10
15
20
25
30
2θ

3

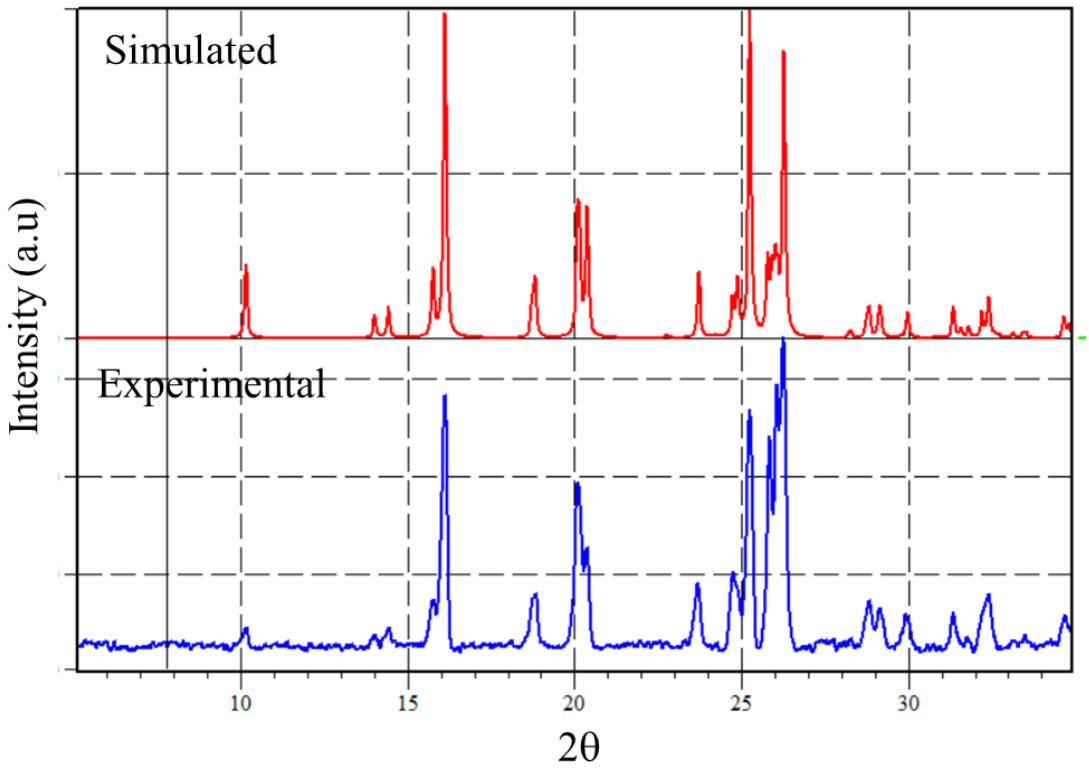
Simulated
Experimental
Intensity (a.u)
10
15
20
25
30
2θ

1.BZA

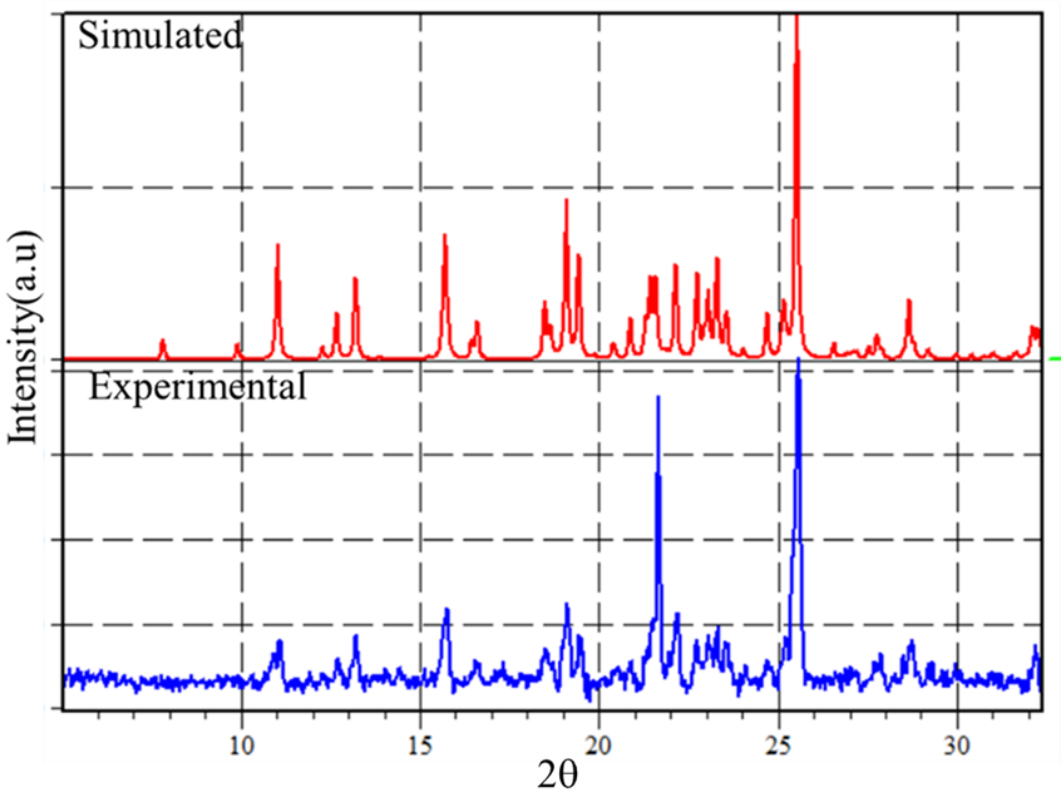
Simulated
Experimental
Intensity(a.u)
10
15
20
25
30
2θ

2.BZA

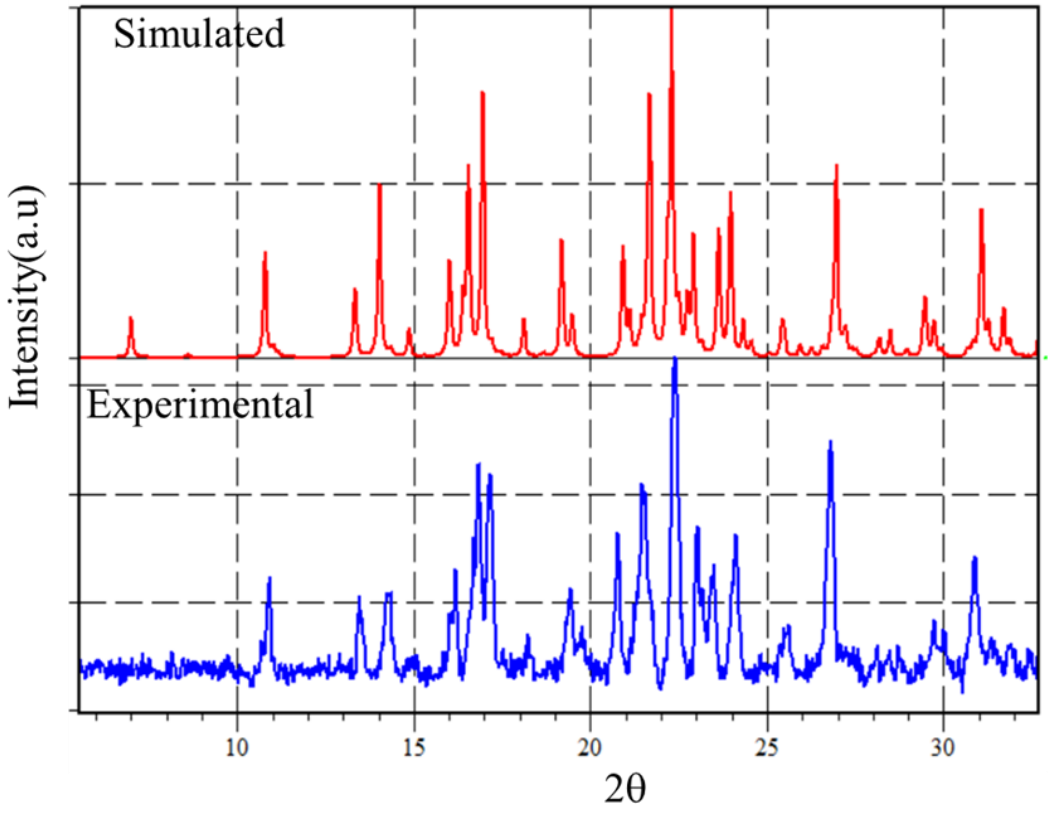
Simulated
Experimental
Intensity(a.u)
10
15
20
25
30
2θ

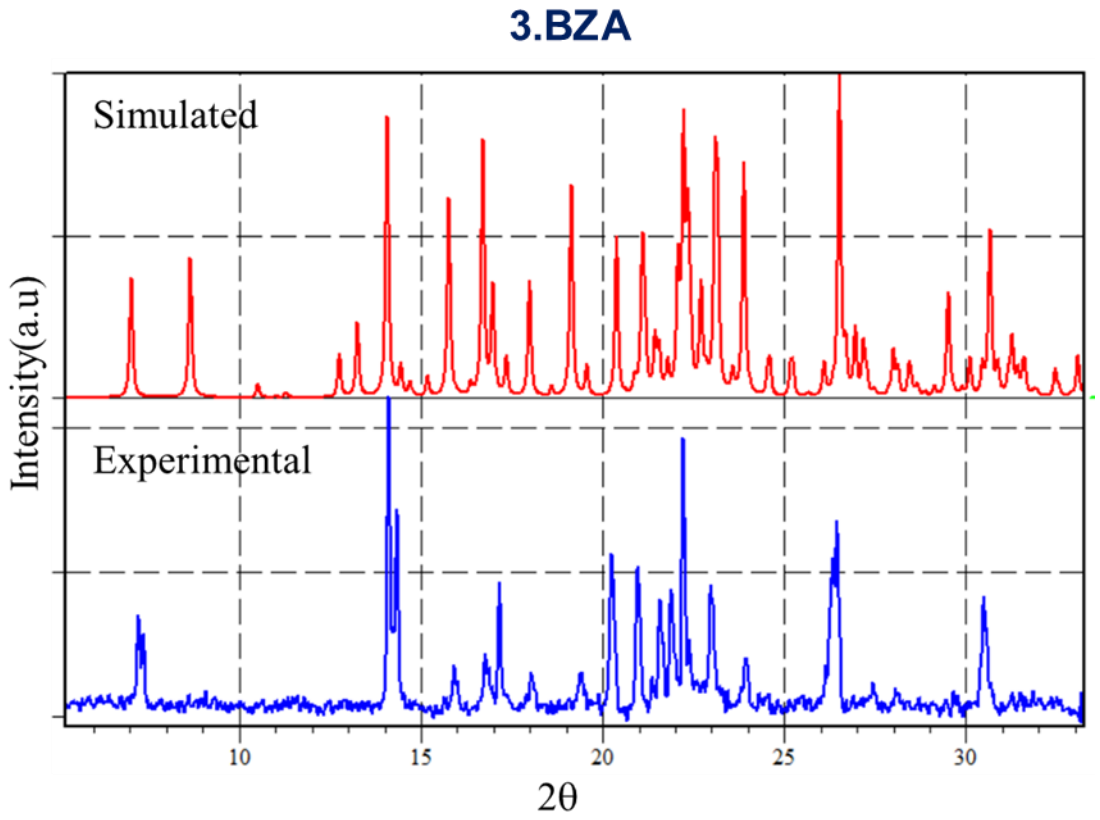

B. Differential Thermal Analysis (DSC):

Samples for DSC were prepared by grinding the recrystallized samples. ~3 mg of samples for both the native and cocrystal system were taken in Al-pans and measured the DSC using Shimadzu DSC-60 instrument within a temperature range of RT to 250° C with a scan rate of 5°C/min.

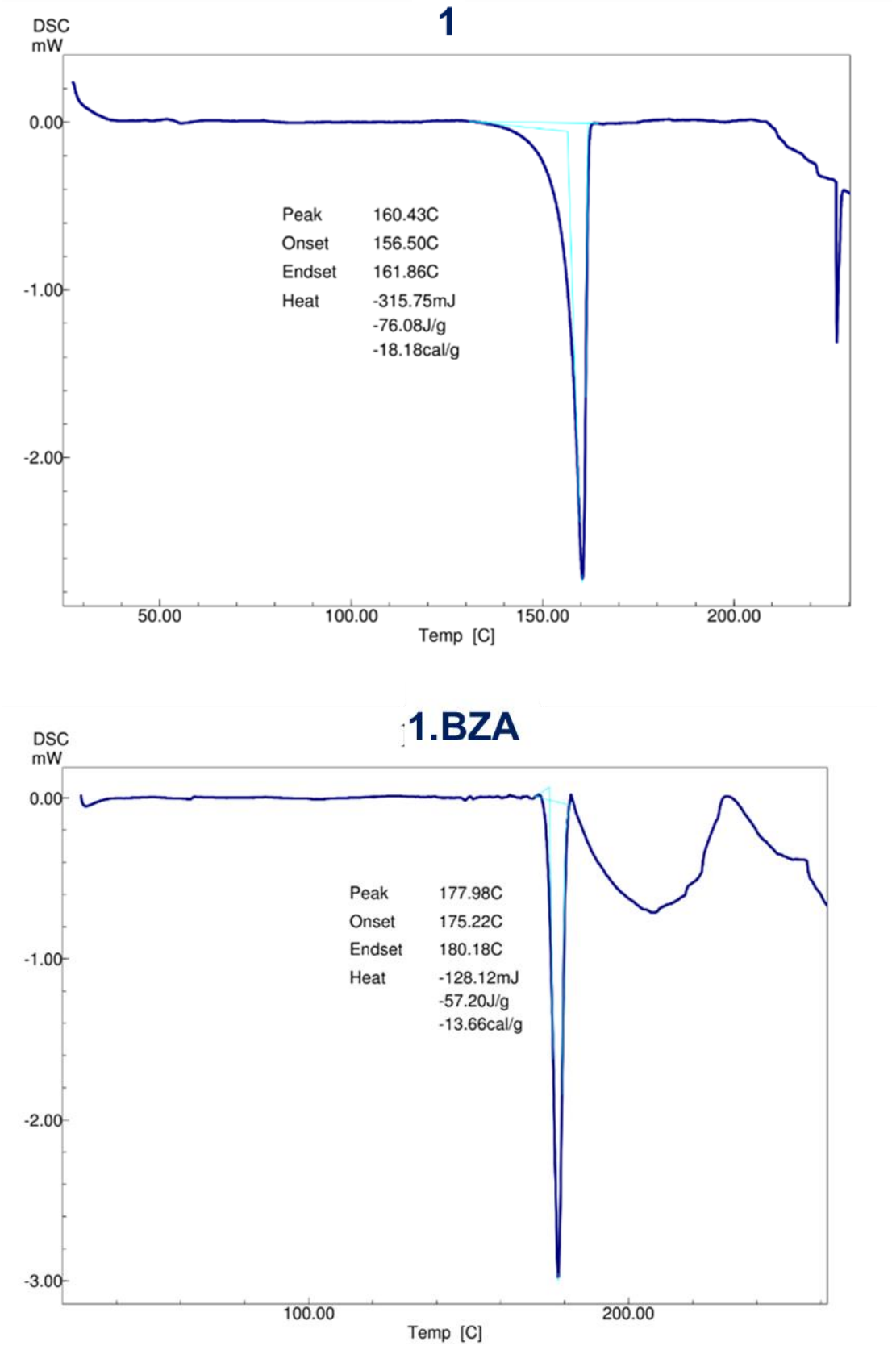

Figure 7: DSC data of 1(top) and 1.BZA (bottom).

S10. Photoirradiation of the compounds and images of irradiated crystals:

Phase pure single crystals were taken in Pyrex glass slides and irradiated using a 450-watt medium-pressure mercury lamp for 12 hours. Pictures of the crystals were collected using the OLYMPUS BX53M microscope before and after irradiation. For 1 and 1.BZA images of the crystals before and after were shown in the manuscript, and for 2,3, 2.BZA and 3.BZA, the pictures of crystals before and after irradiation are shown below.

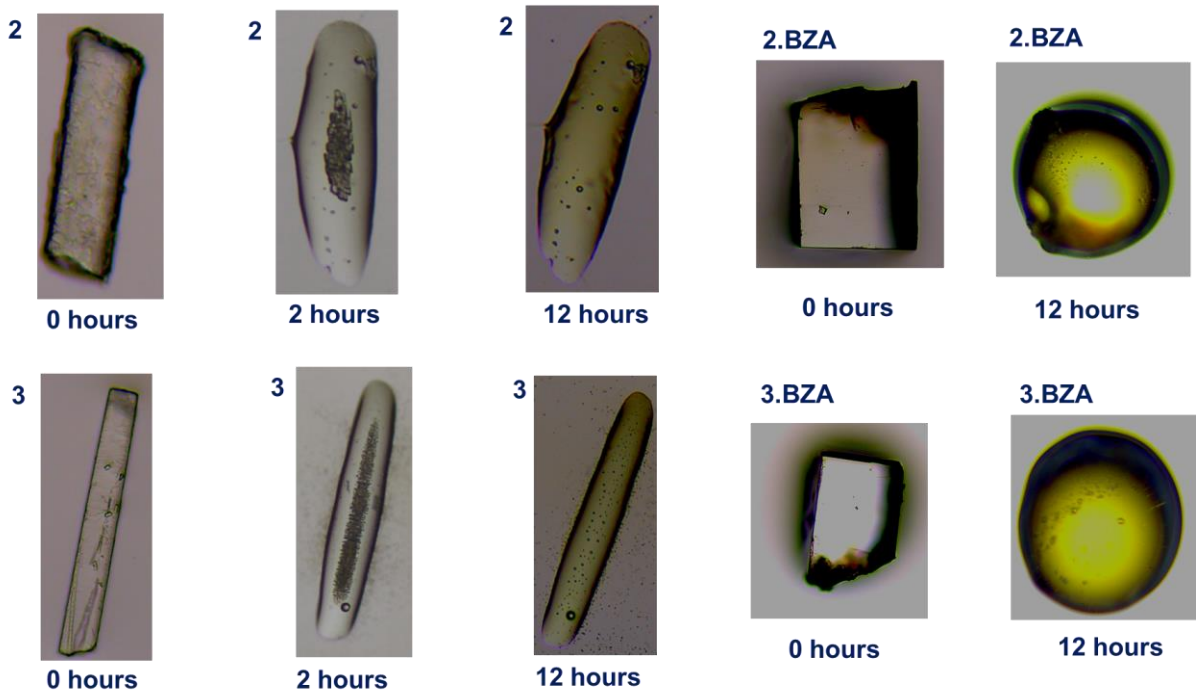

Figure 8. Images of UV-irradiated crystals of 2, 2.BZA; 3 and 3.BZA

S11. ^{1}H NMR characterization of photodimerized products:

A. ^{1}H NMR characterization of 1 after dimerization:

^{1}H NMR for the native compound 1 before and after UV-radiation was collected using Bruker (400 MHz) instrument. ~7 mg of the sample dissolved in $CDCl_3$ for collection of NMR data. If the NMR spectra of before and after irradiation of the compound are compared, an upfield shift was observed for the ortho hydrogen of the pyridine ring due to loss of conjugation. Ortho hydrogen of the 4-styrylpyridine(doublet) is the most downfield H, which shifted from ~8.6 ppm to ~8.44 ppm. and another new peak appeared due to the butane ring formation in the aliphatic region around ~4.39 ppm with coupling constant 7.56 and 2.76 Hz.

1

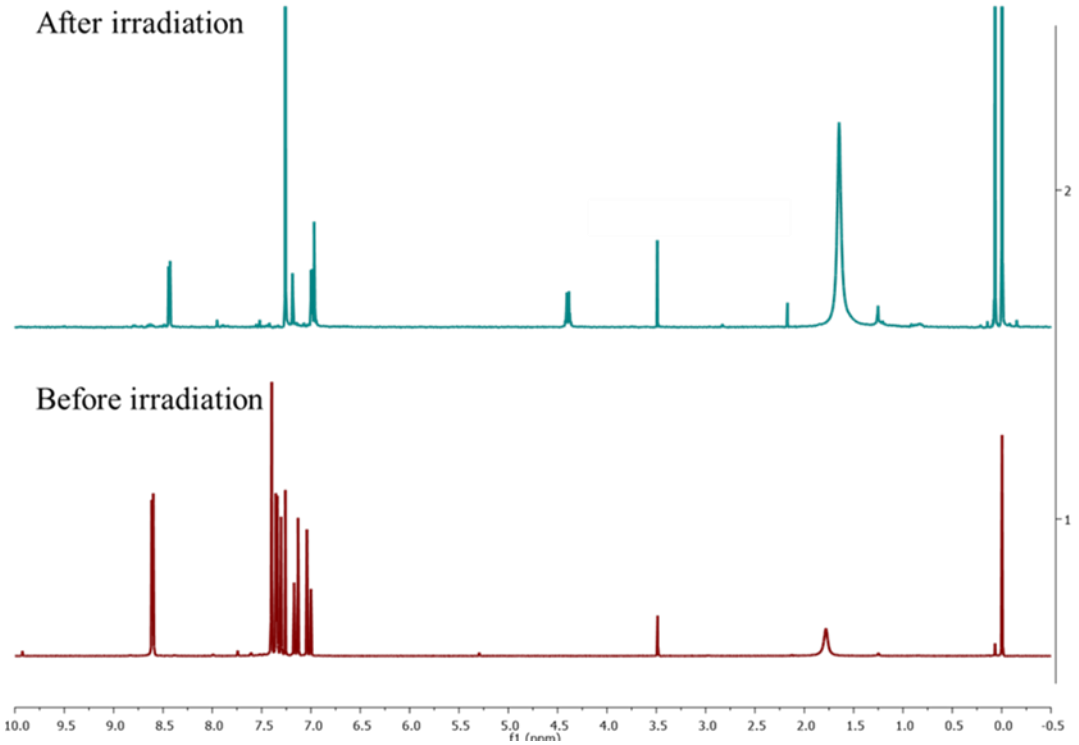
After irradiation
Before irradiation
10.0 9.5 9.0 8.5 8.0 7.5 7.0 6.5 6.0 5.5 5.0 4.5 4.0 3.5 3.0 2.5 2.0 1.5 1.0 0.5 0.0 -0.5
f1 (ppm)

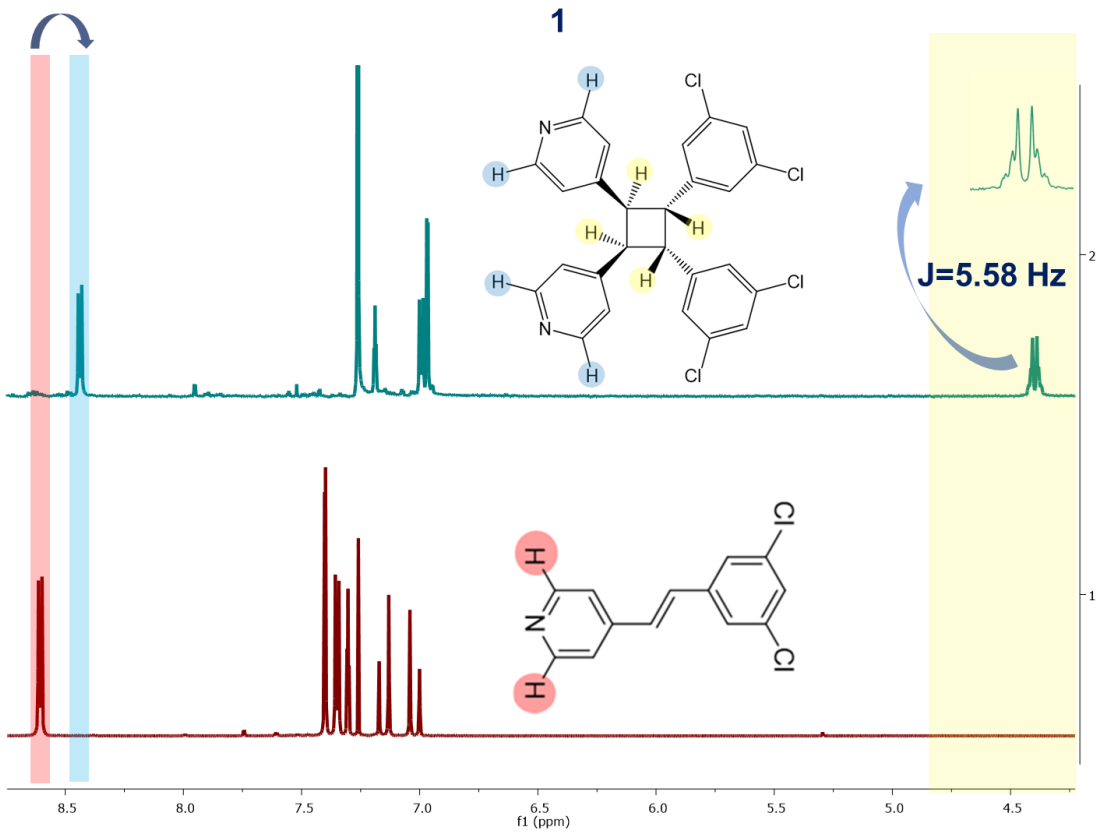
1
J=5.58 Hz
8.5 8.0 7.5 7.0 6.5 6.0 5.5 5.0 4.5
f1 (ppm)

(b) ^{1}H NMR characterization of 1.BZA after dimerization:

^{1}H NMR for 1.BZA before and after UV-radiation was collected using Bruker (400 MHz) instrument. The melted crystals, after irradiation were dissolved in $CDCl_3$, and NMR was for the sample. The most downfield shift at 8.55 ppm was observed for the pyridine ring's ortho hydrogens, which eventually shifted to 8.44 after irradiation. The appearance of a new peak around 4.40 ppm with coupling constants 5.54 Hz and 8.84 Hz confirmed the formation of the dimer.

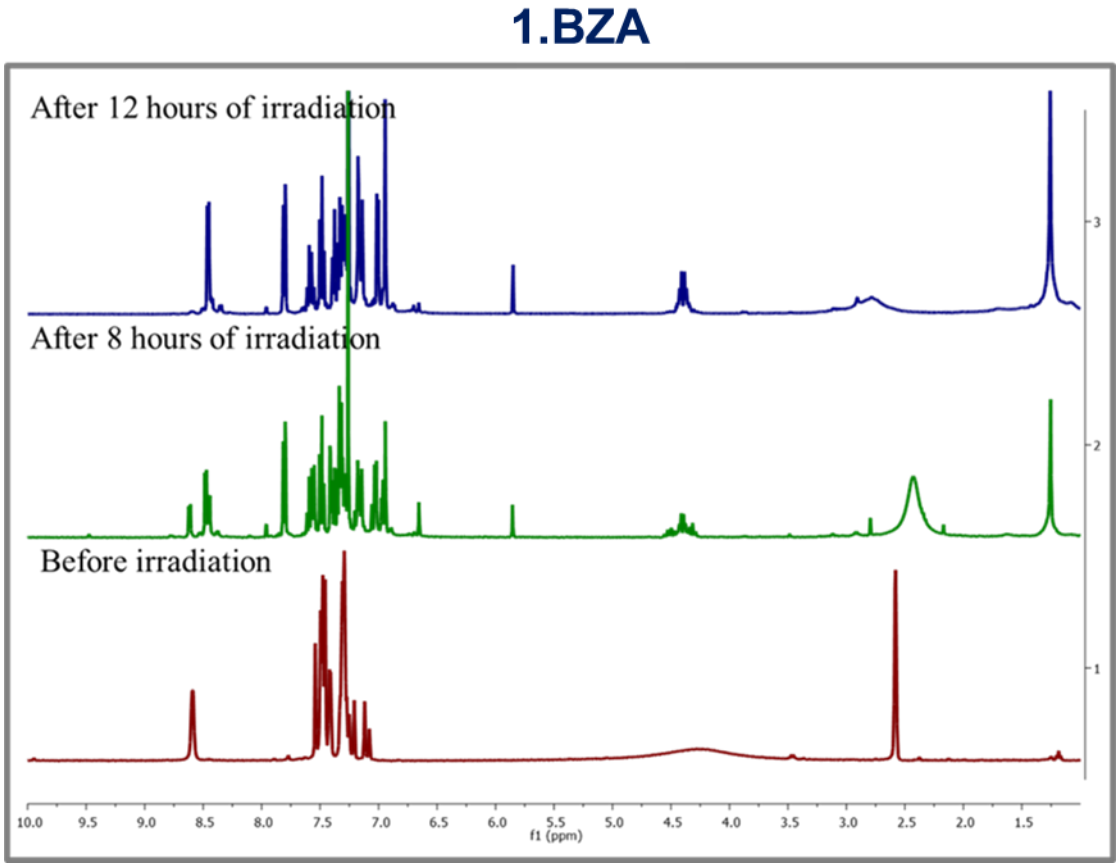

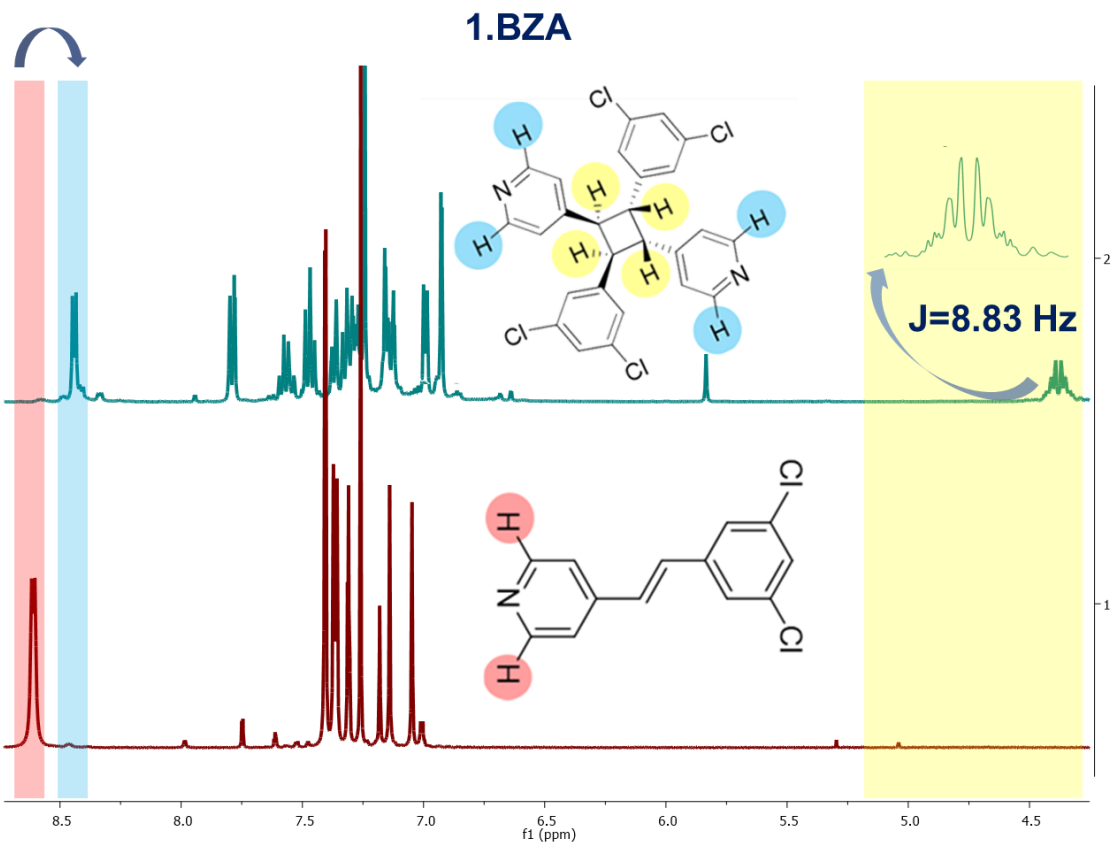

(c) ^{1}H NMR characterization of 2 after dimerization: Melted crystals after irradiation were collected dissolving in $CDCl_3$ using Bruker (400MHz) instrument. Observations form the NMR is discussed below:

1. After 12 hours of irradiation, peak around 8.60(d,6.15 Hz, 2H) (for the ortho hydrogens of pyridine N) did not disappear suggested incomplete conversion to the photo product.

2. Peak around 8.40 (d,6.06 4Hz, 4H) and 4.42 (m, 5.13Hz, 2.99Hz, 4H) appeared after 12 hours of irradiation. These peaks confirm the formation of dimer.

3. Along with dimer new peaks appeared around 8.46 (d, 6.12Hz, 2H) and 6.54(d,12.2Hz and 6.73(d, 12.23Hz). relative intensity of these two peaks were similar this confirms the formation of cis isomer of 2.

4. The relative intensity of the peaks for orthro hydrogens of pyridine ring for trans isomer(2H), cis isomer(2H) and the dimer (4H) was 3.72, 2 and 4.88. When the calculation was done for the irradiated product it was obtained that 45% was unreacted, 25% was the cis isomer and 30% was the dimer product of 2.

5. For native 2 there were two peaks around 7.02 and 7.22 ppm with coupling constant of ~16.33Hz. However, the new peaks around 6.54 and 6.73 ppm with coupling constant of 12.2 Hz confirms the cis isomer formation.

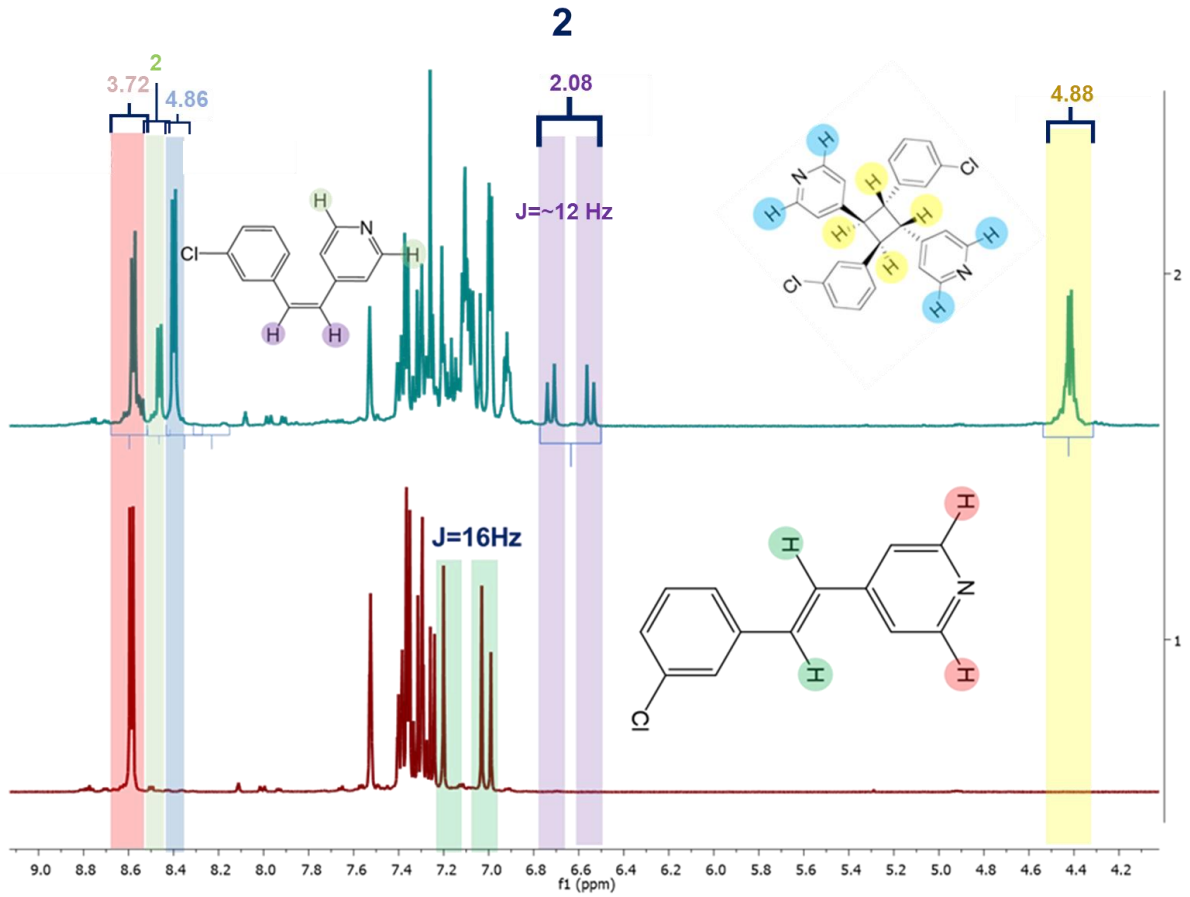

(d) ^{1}H NMR characterization of 2.BZA after dimerization: The melted samples after 8 hours and 12 hours were dissolved in $CDCl_3$ and collected the NMR. Before irradiation, a characteristic peak at 8.62 ppm was observed for ortho hydrogens of the pyridine ring. Careful observation of the NMR data after 8 hours indicates the disappearance of the peak at 8.61 ppm and the appearance of a new peak around 8.44 ppm. The peak at 8.61 ppm completely disappeared after 12 hours of irradiation, with the appearance of a new peak at 8.44 ppm and 4.45 ppm. These two characteristic features confirmed the formation of the dimer upon irradiation.

2.BZA

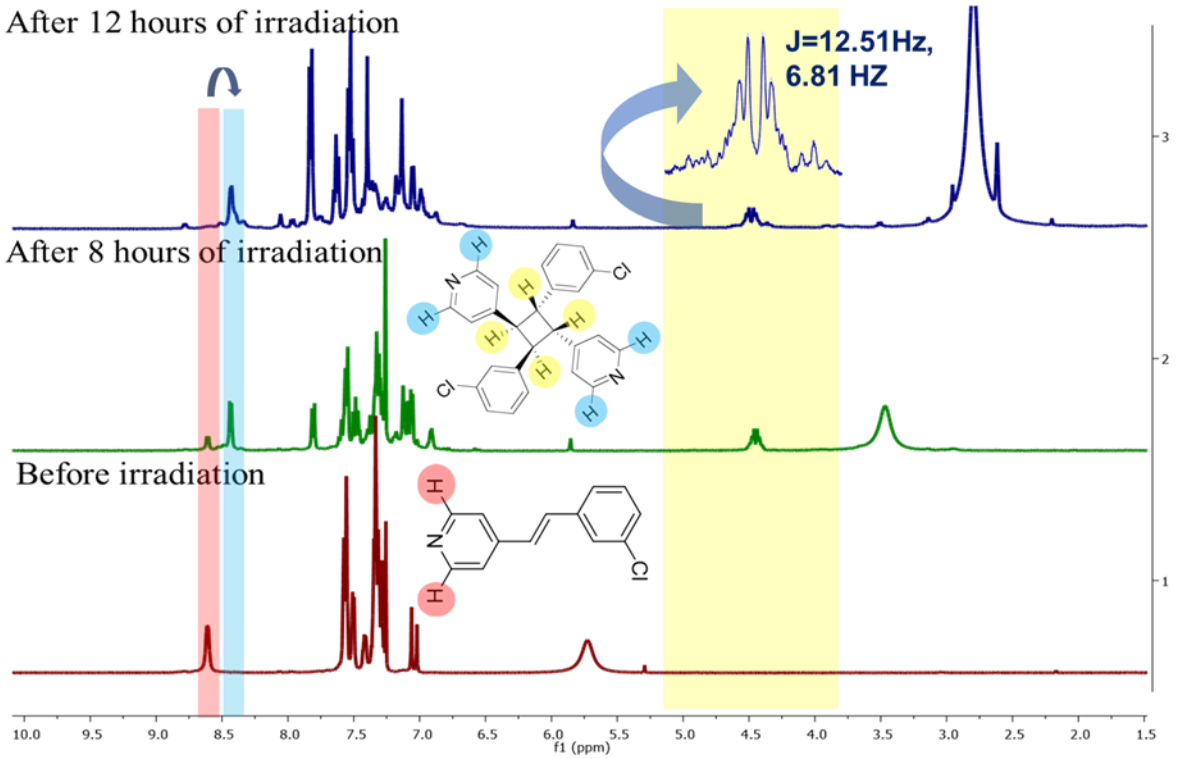

(e) ^{1}H NMR characterization of 3 after dimerization: Melted crystals of 3 were irradiated for 12 hours, irradiated samples were dissolved in $CDCl_3$ and NMR was collected using Bruker (400MHz) instrument. Observations obtained from the NMR is discussed below:

1. When the crystals of 3 were irradiated for 12 hours under UV lamp, peak around 8.58(d,6.31Hz, 2H) (for the ortho hydrogens of pyridine N) confirms the remaining reactant, the trans conformation of 3.

2. Peak around 8.40 (d,6.11Hz, 4H) and 4.42 (m, 4H) appeared after 12 hours of irradiation. These peaks confirm the formation of dimer.

3. Along with dimer new peaks appeared around 8.47 (d, 6.15HZ, 2H) and 6.55(d,12.25Hz and 6.72(d,12.25Hz). Relative intensity of these two peaks were similar this confirms the formation of cis isomer of 3.

4. The relative intensity of the peaks for orhto hydrogens of pyridine ring for trans isomer (2H), cis isomer(2H) and the dimer (4H) was 3.72, 2 and 4.88. When the calculation was done for the irradiated product it was obtained that 26.6 % was unreacted, 13.8% was the cis isomer and 59.6%

% was the dimer product of 3.

5. For native 3 (trans) there were two peaks around 7.02 and 7.22 ppm with coupling constant of ~16.32Hz. However, the new peaks around 6.54 and 6.73 Hz with coupling constant of 12.25 Hz confirms the cis isomer formation.

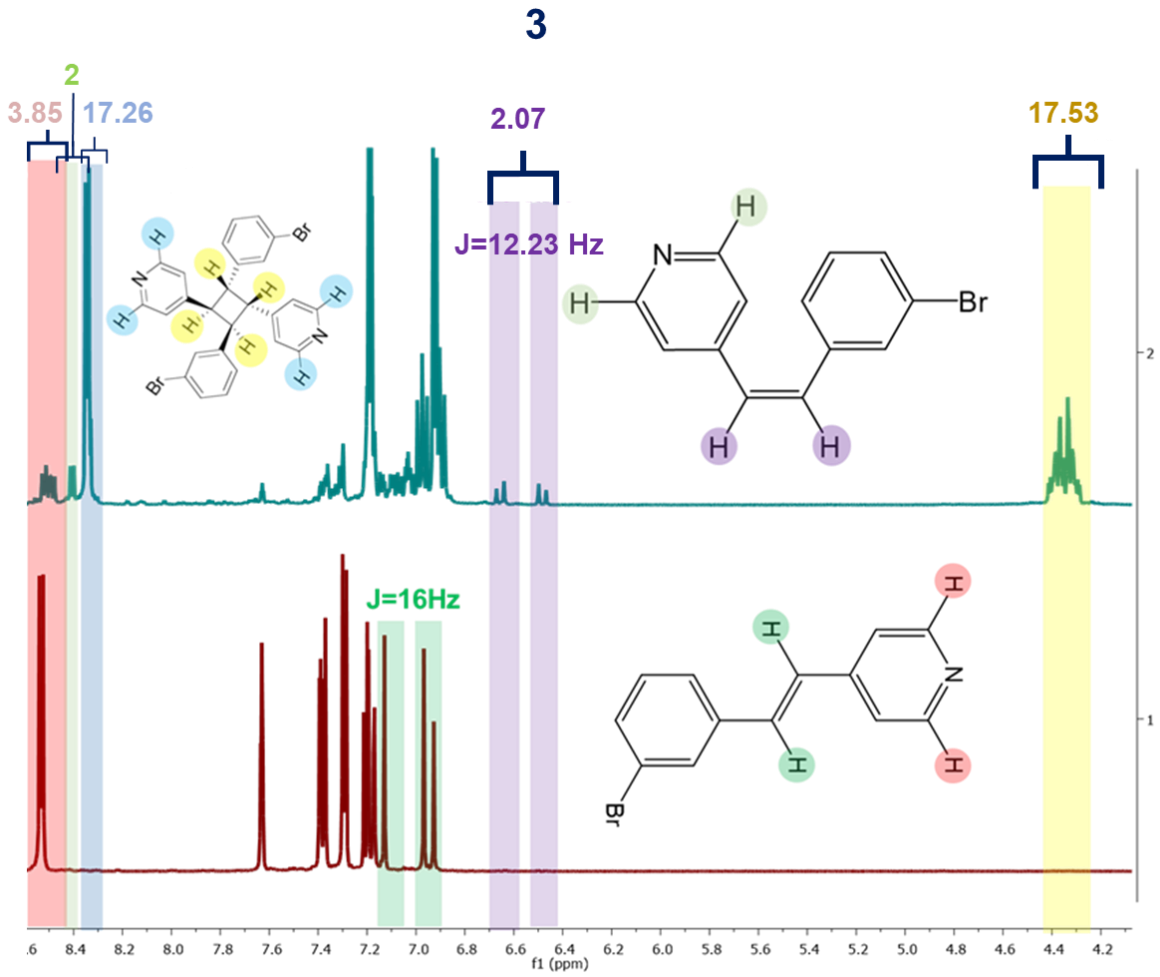

(f) ^{1}H NMR characterization of 3.BZA after dimerization: NMR data of the cocrystal before and after irradiation was collected. 7 mg of the cocrystal before irradiation and the melted samples after 12 hours of irradiation were dissolved in $CDCl_3$ and collected the NMR. Before irradiation, a characteristic peak at 8.6 was observed for ortho hydrogens of the pyridine ring, which shifted to 8.4 ppm after irradiation. New peaks around 4.45 ppm appeared, which confirmed the formation of the dimer.

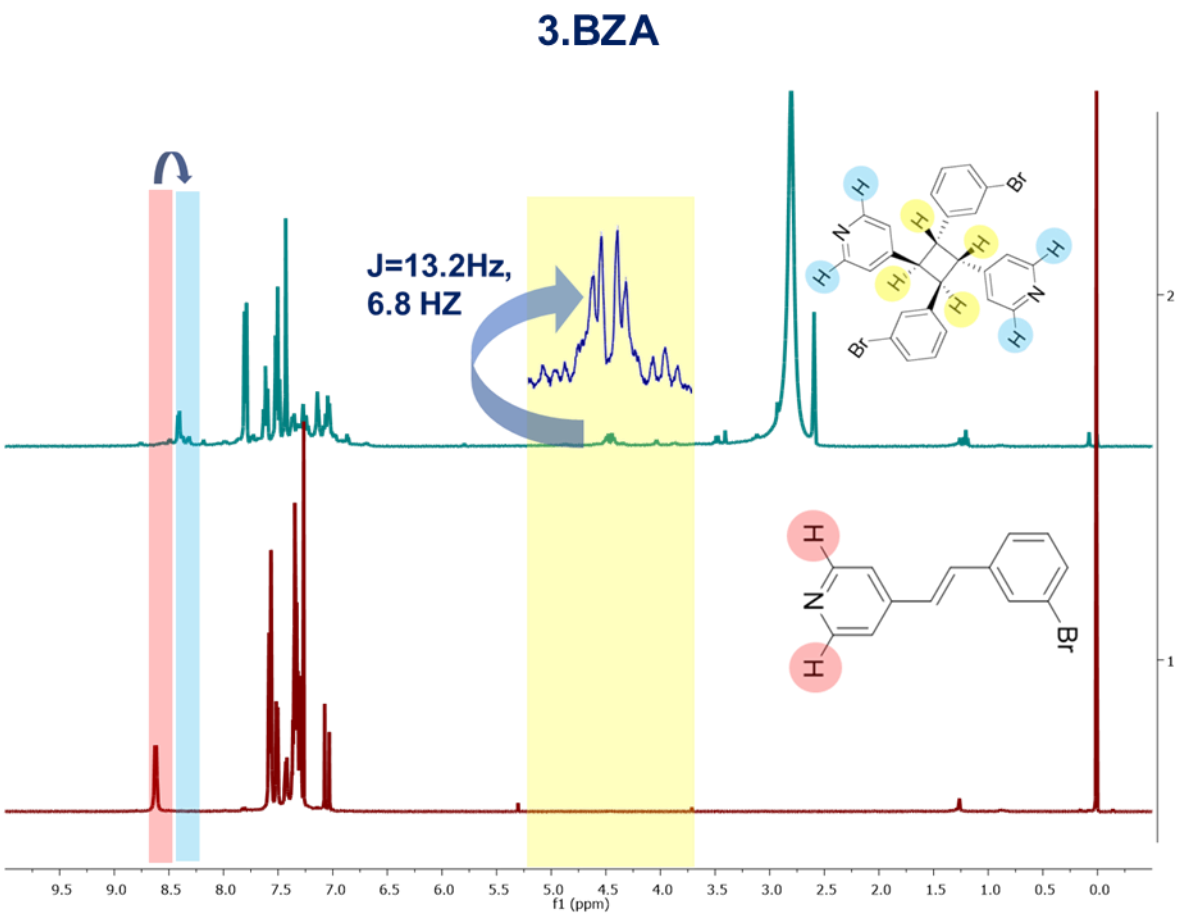

B. ^{13}NMR of photodimerization.

^{13}C NMR for the native compound and cocrystal before and after UV-radiation was collected using AV NEO (100 MHz). 7 mg of the sample before irradiation, 5 mg of sample 1, and melted form of 1.BZA were dissolved in $CDCl_3$ to collect NMR data. The appearance of new peaks around 44 ppm in the irradiated samples confirmed the dimer formation.

1

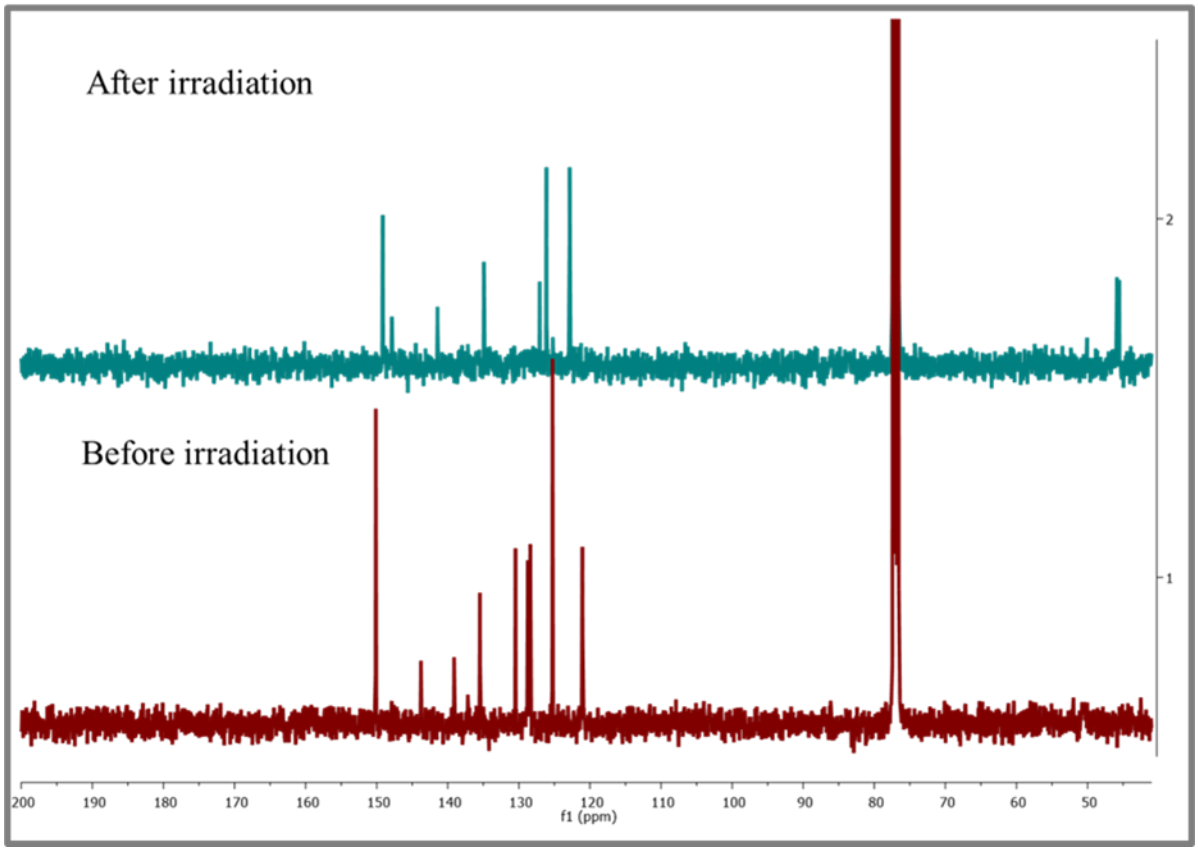
After irradiation
Before irradiation
2
1
200
190
180
170
160
150
140
130
120
110
100
90
80
70
60
50
f1 (ppm)

1.BZA

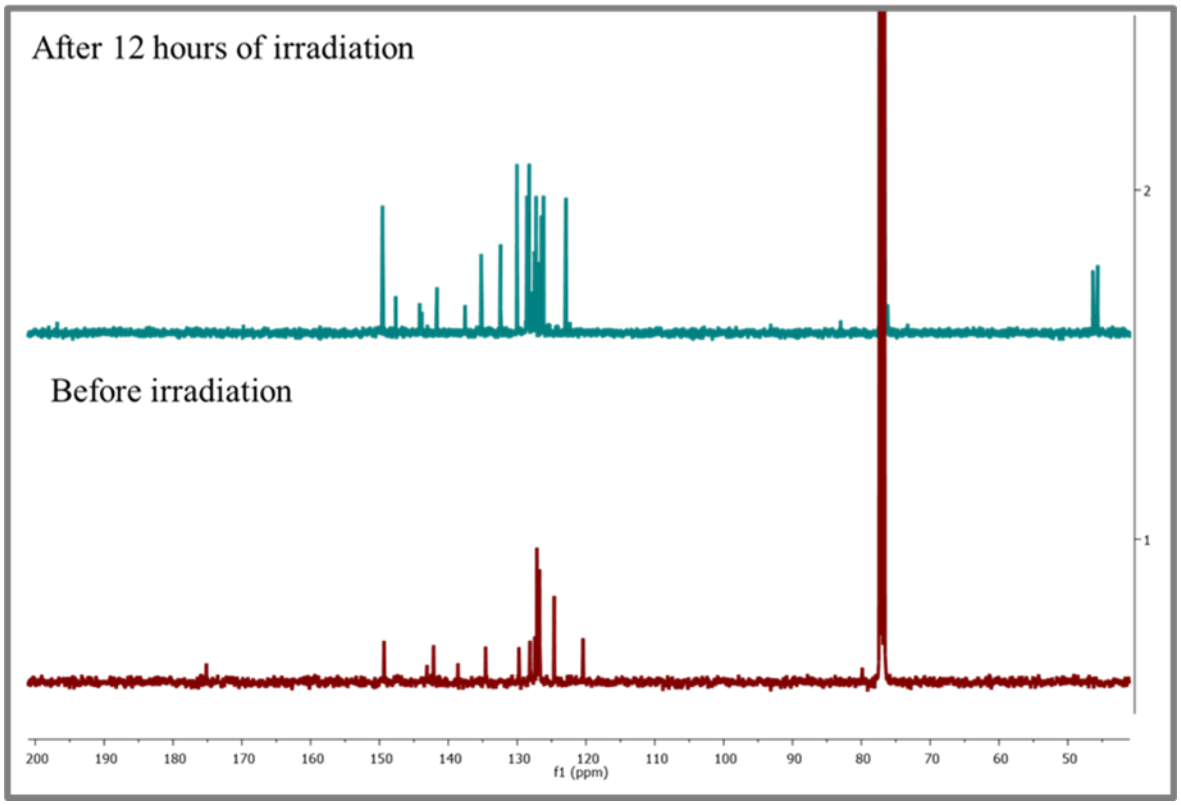

Figure 9: Stacked ^{13}C NMR spectra before and after irradiation of 1 (top) 1.BZA (bottom)

C. Mass spectra of the compound before and after irradiation:

Mass spectra of the compounds before and after irradiation were collected by dissolving a pinch of compound in methanol. The appearance of a peak at 501 in irradiated samples confirms the formation of the dimer of 1.BZA. The appearance of a new peak around 431 confirmed the formation of the dimer of 2.BZA upon irradiation and peak appearance around 520 confirmed the dimer formation of 3.BZA upon irradiation. For 1.BZA and 2.BZA, another peak around 432 and 400, appeared with an abundance of nearly 50 % after dimerization. These two peaks in the respective structures come due to the α-cleavage of two chlorine atoms in 1.BZA and α-cleavage of 1 chlorine atom in 2.BZA.

1.BZA

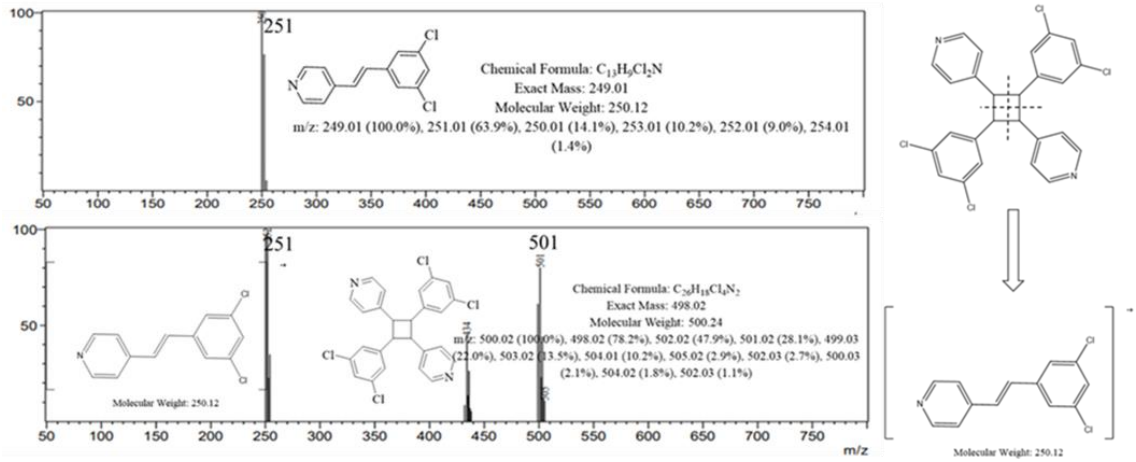

2.BZA

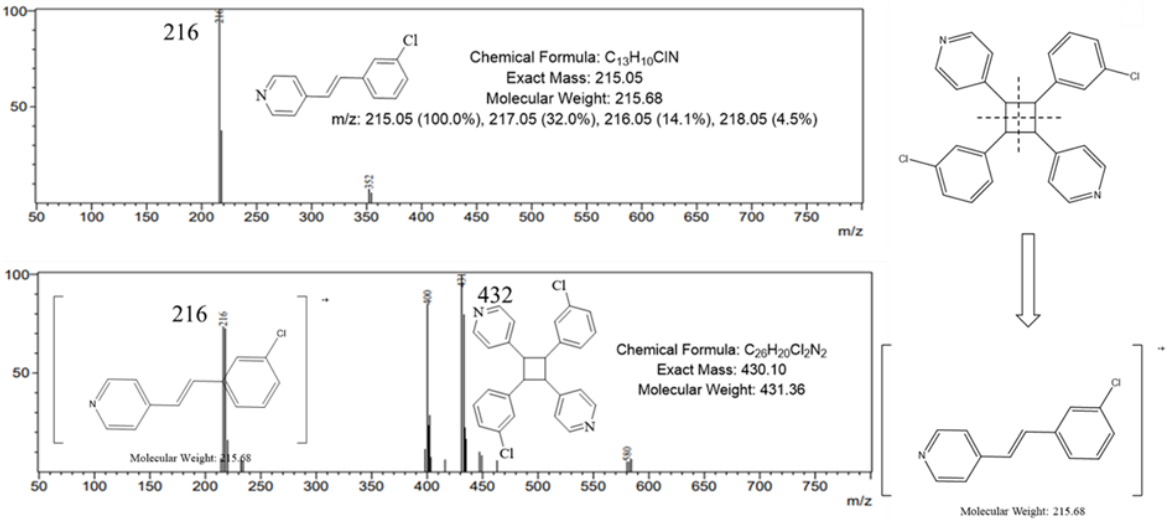

3.BZA

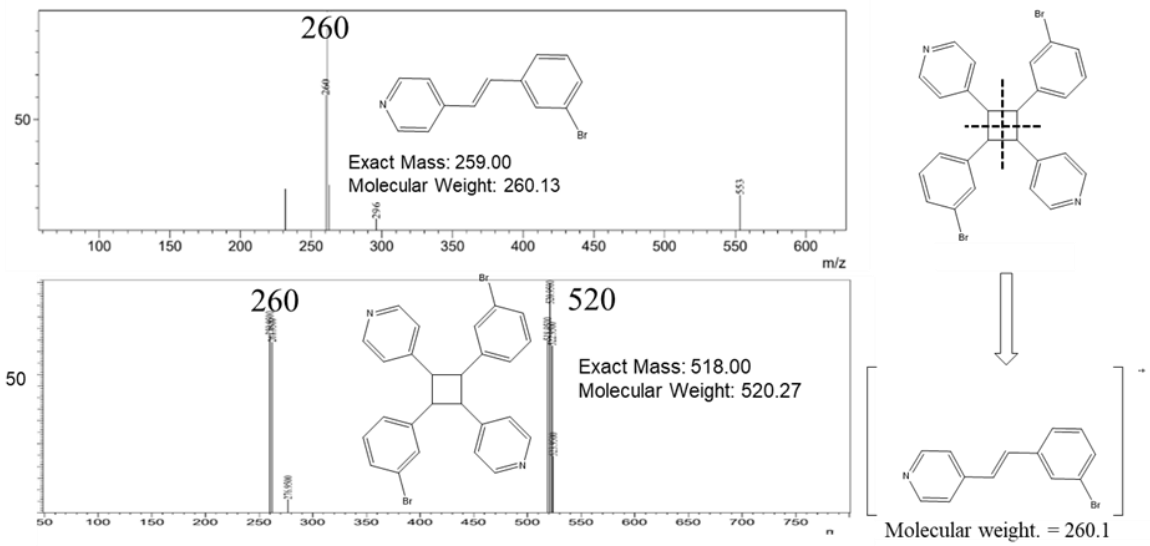

Figure 10: Stacked Mass spectra before and after irradiation of 1.BZA., 2.BZA, and 3.BZA. The fragmentation is shown in the right, defining the appearance of two significant peaks after irradiation.

S12. Response to A and B alerts:

start Validation Reply Form for **2.BZA**

_vrf_PLAT353_exp_1320_am-r-135-can;

PROBLEM: Long N-H (N0.87,N1.01A) N5 - H2 . 1.10 Ang.

RESPONSE: ...Δpk_a calculation results for the system indicate possible salt formation. Therefore, the N-H bond length was higher than the normal bond length, that is why this B alert was generated.

_vrf_PLAT772_exp_1320_am-r-135-acn;

PROBLEM: Suspect O-H Bond in CIF: O2 --H2 .. 1.46 Ang.

RESPONSE: ...Δpk_a calculation results for the system indicate possible salt formation. For that reason, it showed a possibility of O-H bond formation. Due to this reason, this B alert was generated.

end Validation Reply Form

S13. ORTEP Diagrams:

ORTEP diagrams were created using a 50% probability.

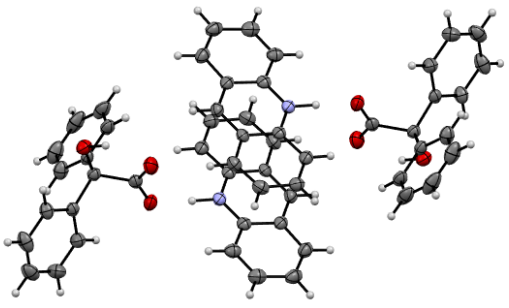	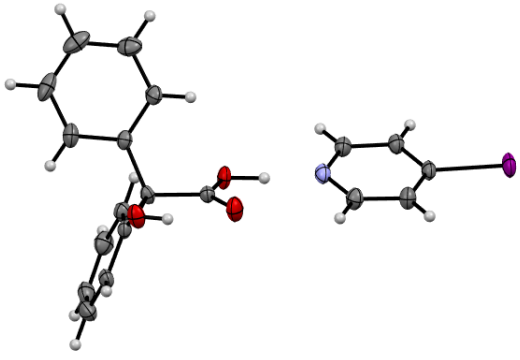
BZA-ACR	*BZA-4IPy*

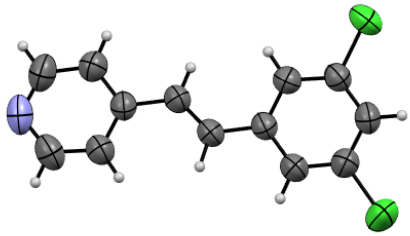	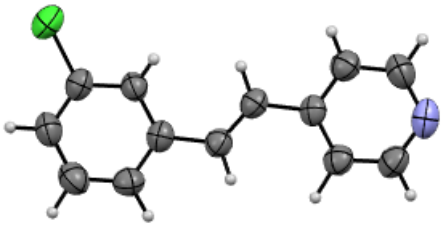
1	*2*

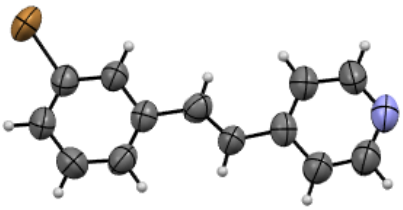	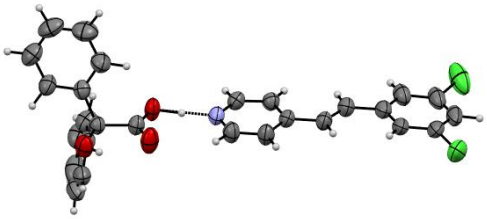
3	*1.BZA*

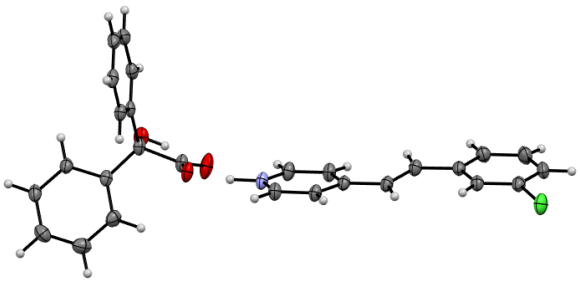	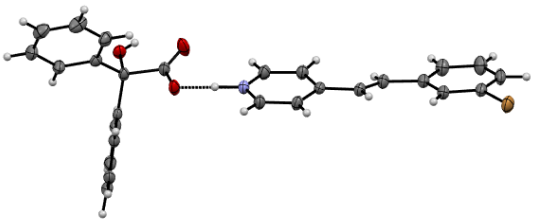
2.BZA	*3.BZA*

References:

1 A. I. Vogel and B. S. Furniss, *Vogel's Textbook of practical organic chemistry*, Longman Scientific & Technical ; Wiley London, New York, London, New York, 5th ed., 1989.

2 J. L. R. Williams, R. E. Adel, J. M. Carlson, G. A. Reynolds, D. G. Borden and J. A. Ford, *J. Org. Chem.*, 1963, **28**, 387–390.

3 B. R. Bhogala, B. Captain, A. Parthasarathy and V. Ramamurthy, *J. Am. Chem. Soc.*, 2010, **132**, 13434–13442.

4 E. Elacqua, P. Kaushik, R. H. Groeneman, J. C. Sumrak, D.-K. Bučar and L. R. MacGillivray, *Angew. Chem. Int. Ed.*, 2012, **51**, 1037–1041.

5 E. Elacqua, K. A. Kummer, R. H. Groeneman, E. W. Reinheimer and L. R. MacGillivray, *J. Photochem. Photobiol. Chem.*, 2016, **331**, 42–47.

6 B. R. Bhogala, B. Captain and V. Ramamurthy, *Photochem. Photobiol.*, 2015, **91**, 696–704.
7 M. A. Sinnwell, R. H. Groeneman, B. J. Ingenthron, C. Li and L. R. MacGillivray, *Commun. Chem.*, 2021, **4**, 60.
8 S. Dutta, D.-K. Bučar and L. R. MacGillivray, *Org. Lett.*, 2011, **13**, 2260–2262.
9 D.-K. Bučar, A. Sen, S. V. S. Mariappan and L. R. MacGillivray, *Chem. Commun.*, 2012, **48**, 1790.
10 E. Bosch, S. J. Kruse, E. W. Reinheimer, N. P. Rath and R. H. Groeneman, *CrystEngComm*, 2019, **21**, 6671–6675.
11 S. M. Oburn, M. A. Sinnwell, D. P. Ericson, E. W. Reinheimer, D. M. Proserpio, R. H. Groeneman and L. MacGillivray, *IUCrJ*, 2019, **6**, 1032–1039.
12 A. L. Grobelny, N. P. Rath and R. H. Groeneman, *Photochem. Photobiol. Sci.*, 2019, **18**, 989–992.
13 A. L. Grobelny, N. P. Rath and R. H. Groeneman, *CrystEngComm*, 2018, **20**, 3951–3954.
14 G. Campillo-Alvarado, K. P. D'mello, D. C. Swenson, S. V. Santhana Mariappan, H. Höpfl, H. Morales-Rojas and L. R. MacGillivray, *Angew. Chem. Int. Ed.*, 2019, **58**, 5413–5416.
15 G. Campillo-Alvarado, C. Li, Z. Feng, K. M. Hutchins, D. C. Swenson, H. Höpfl, H. Morales-Rojas and L. R. MacGillivray, *Organometallics*, 2020, **39**, 2197–2201.
16 L. R. MacGillivray, J. L. Reid and J. A. Ripmeester, *J. Am. Chem. Soc.*, 2000, **122**, 7817–7818.
17 G. Ortega, J. Hernández, T. González, R. Dorta and A. Briceño, *Photochem. Photobiol. Sci.*, 2018, **17**, 670–680.
18 S. Li and D. Yan, *ACS Appl. Mater. Interfaces*, 2018, **10**, 22703–22710.
19 S. Li, B. Lu, X. Fang and D. Yan, *Angew. Chem. Int. Ed.*, 2020, **59**, 22623–22630.
20 S. P. Yelgaonkar, D. Kiani, J. Baltrusaitis and L. R. MacGillivray, *Chem. Commun.*, 2020, **56**, 6708–6710.
21 T. B. Nguyen, T. M. Nguyen and P. Retailleau, *Chem. – Eur. J.*, 2020, **26**, 4682–4689.
22 C. Li, G. Campillo-Alvarado, D. C. Swenson and L. R. MacGillivray, *CrystEngComm*, 2021, **23**, 1071–1074.
23 A. J. Cruz-Cabeza, M. Lusi, H. P. Wheatcroft and A. D. Bond, *Faraday Discuss.*, 2022, **235**, 446–466.
24 L. J. Farrugia, *J. Appl. Crystallogr.*, 1999, **32**, 837–838.
25 P. R. Spackman, M. J. Turner, J. J. McKinnon, S. K. Wolff, D. J. Grimwood, D. Jayatilaka and M. A. Spackman, *J. Appl. Crystallogr.*, 2021, **54**, 1006–1011.
26 C. F. Macrae, I. Sovago, S. J. Cottrell, P. T. A. Galek, P. McCabe, E. Pidcock, M. Platings, G. P. Shields, J. S. Stevens, M. Towler and P. A. Wood, *J. Appl. Crystallogr.*, 2020, **53**, 226–235.